SILOXANE SCINTILLATOR

Drs. J. Harmon and J. Walker
University of Florida

Siloxanes were first irradiated by the Detector Development Group at the University of Florida. We present those results.

One centimeter thick samples of several commercial plastics were irradiated using a ^{60}Co radioactive source. In addition, we exposed a sample of polysiloxane plastic with the same dimensions. The optical transmission of the samples was measured after 10^7 Rads of irradiation with ^{60}CO gamma rays. Early results of these studies are shown in Figure 1A for the case where all the samples were maintained in an air atmosphere throughout the irradiation. The fact that the optical transmissions are measured to be less than 100% is due to surface reflections by the sample and not bulk attenuation. Similar, more recent measurements for polysiloxane are shown in more detail in Figure 1B. It should be emphasized that our objective for a plastic scintillation counter is transmission of light over a distance of at least three meters in the plastic. Hence, even small (~2%) radiation effects on the transmission at the desired wavelength with the 1 cm samples must be regarded as extremely serious. These transmission measurements were made immediately following the radiation exposure which took place at 120,000 Rads/hour. The following remarks should be made:

1. The polysiloxane shows $\leq 0.5\%$ loss in transmission for ≥ 500 nm wavelengths per cm of pathlength. This corresponds to an attenuation length of 2 meters after an exposure of 10 Mega Rads. If there is any long term annealing affect

then the attenuation length after irradiation will be even longer than 2 meters. Over a short period (2 months) we have not observed any significant annealing of polysiloxane. We also do not observe significantly different results using different phenyl content siloxanes.

2. All other polymers exhibit large ≥10% loss of transmission at the same wavelength of 500 nm and a reducing loss at increasing wavelength.

3. With the passage of time the transmission loss of the other polymers diminishes (annealing effect) but at any given wavelength reaches an irreducible limit. For example, a 1 cm sample of polystyrene anneals to a permanent loss in transmission of 5% at 500 nm and about 4% at 600 nm after 10 months. (Results presented by Dr. R. Clough at this Workshop). This is a factor of ten larger transmission loss at 500 nm than in the case of polysiloxane. In addition, there may be some slight annealing effect with polysiloxane which would further enhance the difference between siloxane and polystyrene. This result for polystyrene produces an attenuation length of about 20 cm after 10 Megarads. Measurements (after annealing) with polystyrene fibers doped with 3HF, which emits at about 520 nm, indicate attenuation lengths consistent with this figure. This is considered unacceptable for use at the SSC.

The above considerations on the large differences in polysiloxane and polystyrene attenuation lengths are the fundamental technical justifications for the importance of proceeding with polysiloxane fibers for the SSC. This substantial difference in radiation

induced light transmission is probably linked to the difference in atomic valence structure along the back-bone of siloxane compared to any of the carbon based polymers. In the latter case, double bonds can be made to form and, as the integrated radiation dose increases, an expanding region of conjugation can develop. This can produce light absorption, first in the blue and then progressively towards longer wavelengths. In the case of siloxane polymer, the oxygen atom with valence two prohibits the formation of a region of conjugation along the back-bone. We believe it is this fundamental prohibition of extended conjugation in siloxane which confers it with superior resistance to optical degradation.

A further slight improvement in the radiation stability of the polysiloxane is achieved by maintaining an argon environment during the irradiation. In this case there is acceptably small absorption at greater than about 480 nm for 10 Mrads exposure. Hence, a single secondary fluor may be adequate to shift the fluorescent light up to > 480 nm and transport it efficiently over long distances. In the previous cast of the detector operating in air a tertiary fluor must be added to wavelength shift up to > 500 nn. Alternatively, a single dye (eg 3HF) with large stokes shift may be used.

We conducted light output studies on a random dimethyl diphenyl siloxane containing 37 mole % diphenyl and standard polystyrene based scintillator. In order to examine the effect of dye concentration on light output, thin films were cast containing different weight percentages of 3HF. The minimum film thickness for Americium α-particle containment was determined, then dye concentration effects were measured.

Measurements were made in a light proof box into which a photomultiplier tube (RCA Model 8850, ten stages) had been installed. Type 68 adhesive (Norland Products, Inc.) was

used to affix samples to the phototube. The sources were ^{207}Bi and ^{241}Am. An Ortec Model 556 Power Supply was used for the phototube and a LeCroy qvt was used for pulse height analysis.

In the case of 100 μm diameter fibers, used for particle tracking at the SSC, it is necessary to employe only a single fluor with very large stokes shift. Otherwise, the required concentration of the secondary/tertiary fluors is so high that severe self absorption of the transmitted light would occur along the length of the fiber. It is, therefore, generally acknowledged that an intra-molecular proton transfer fluor, such as 3HF, is the optimum fluor for this application at the SSC. 3HF was incorporated into PS and siloxane by dissolving polymer and dye in methylene chloride. Films were made on glass slides with a doctor blade. At thicknesses from 1-5 mil, light output was constant indicating that α-particles were stopped at ranges ≤1 mil. Figure 3 is a plot of light output versus 3HF concentration for PS and siloxane. Results are essentially identical for siloxane and PS. This indicates that high phenyl content siloxane is comparable to PS (standard scintillator bases) in light output. Finally, we show in Figure 4 results on the stability of light output versus radiation dose on a 1 cm^3 siloxane plastic scintillator. In this case, a quarterphenyl primary fluor and TPB secondary fluor were used. Results with a commercial polystyrene based scintillator are also shown.

All of these results confirm that we can produce a radiation hard, high light output scintillating fiber for operation at the SSC.

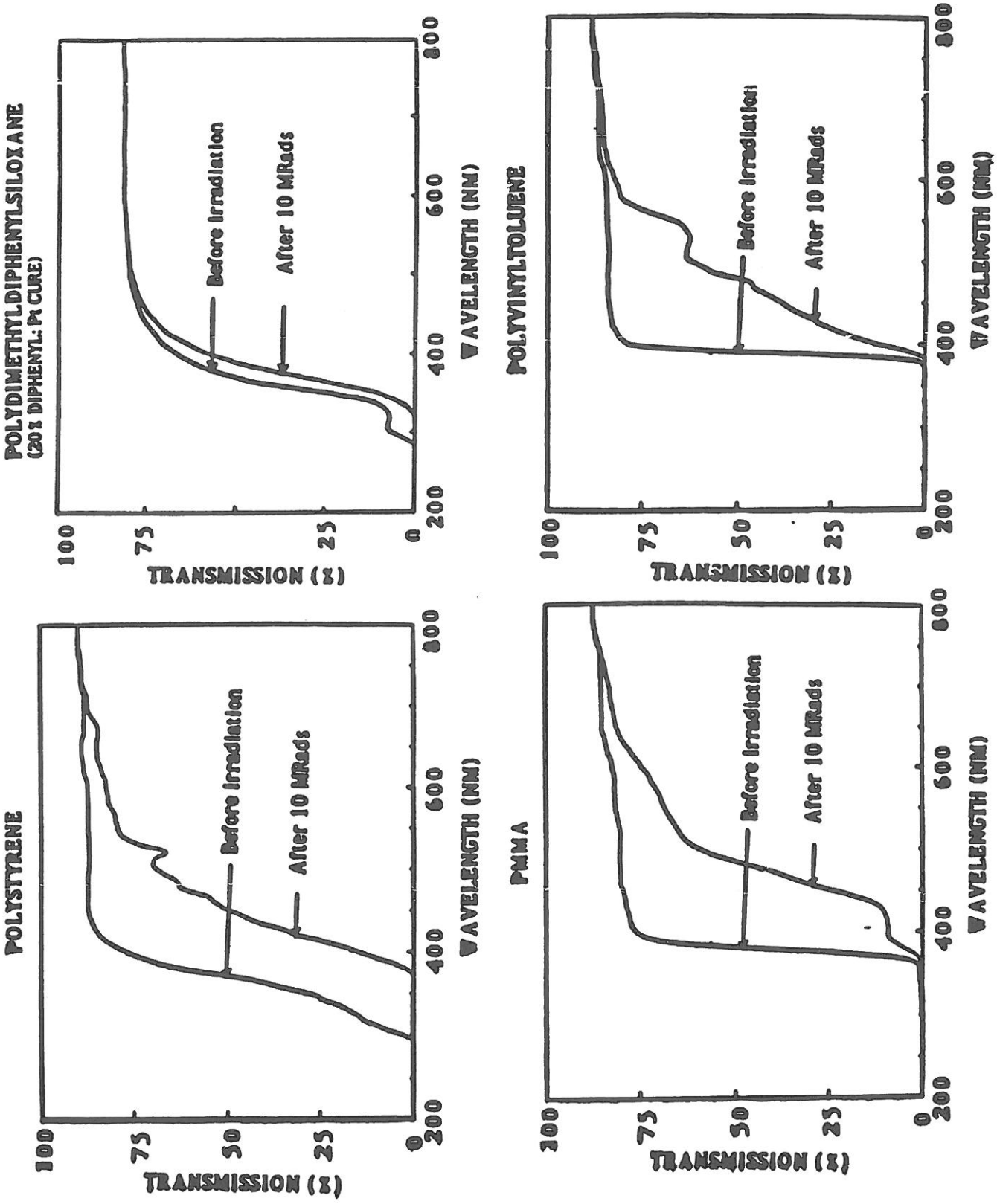
POLYDIMETHYLDIPHENYLSILOXANE
(20% DIPHENYL: Pt CURE)
POLYSTYRENE
POLYVINYLTOLUENE
PMMA
Before Irradiation
After 10 MRads
TRANSMISSION (%)
WAVELENGTH (NM)
100
75
50
25
0
200
400
600
800

FIGURE 1a.

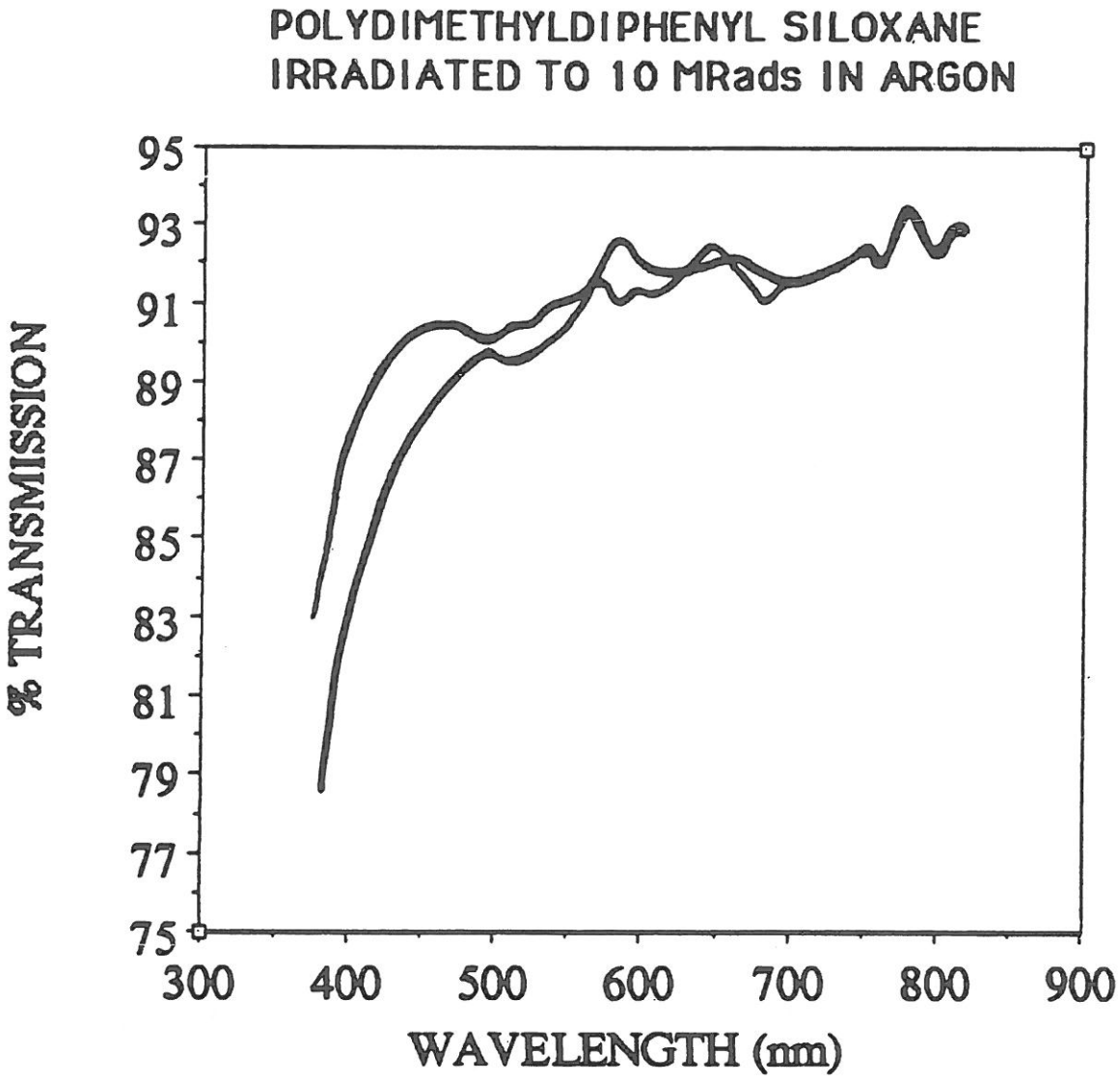
POLYDIMETHYLDIPHENYL SILOXANE
IRRADIATED TO 10 MRads IN ARGON
% TRANSMISSION
95
93
91
89
87
85
83
81
79
77
75
300
400
500
600
700
800
900
WAVELENGTH (nm)

FIGURE Ib

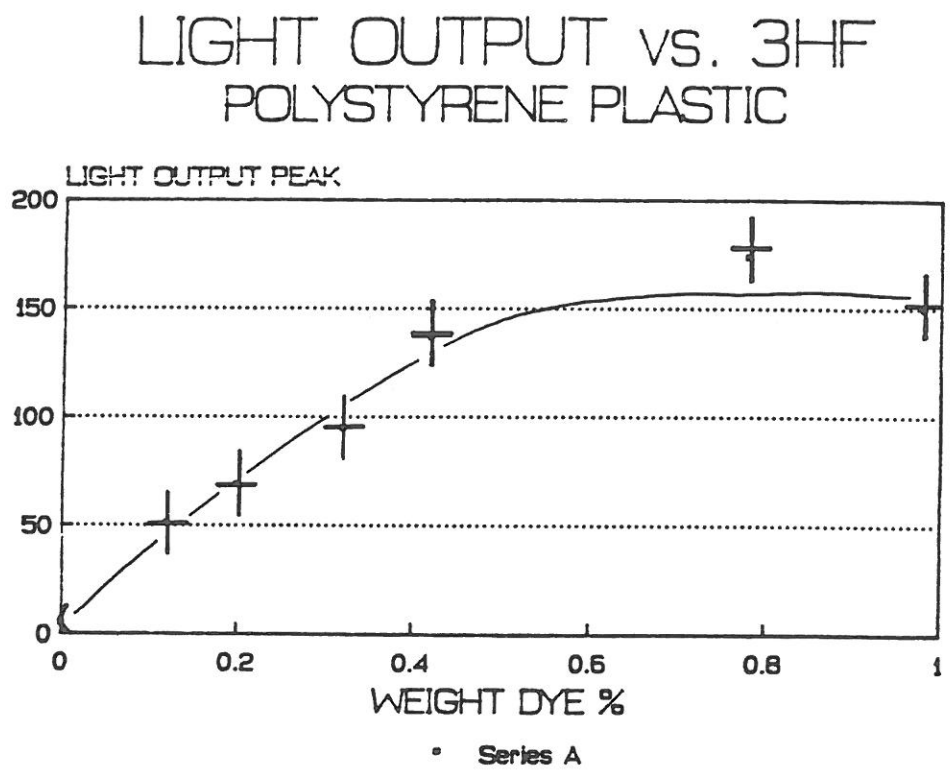
LIGHT OUTPUT vs. 3HF
POLYSTYRENE PLASTIC
LIGHT OUTPUT PEAK
200
150
100
50
0
0
0.2
0.4
0.6
0.8
1
WEIGHT DYE %
Series A

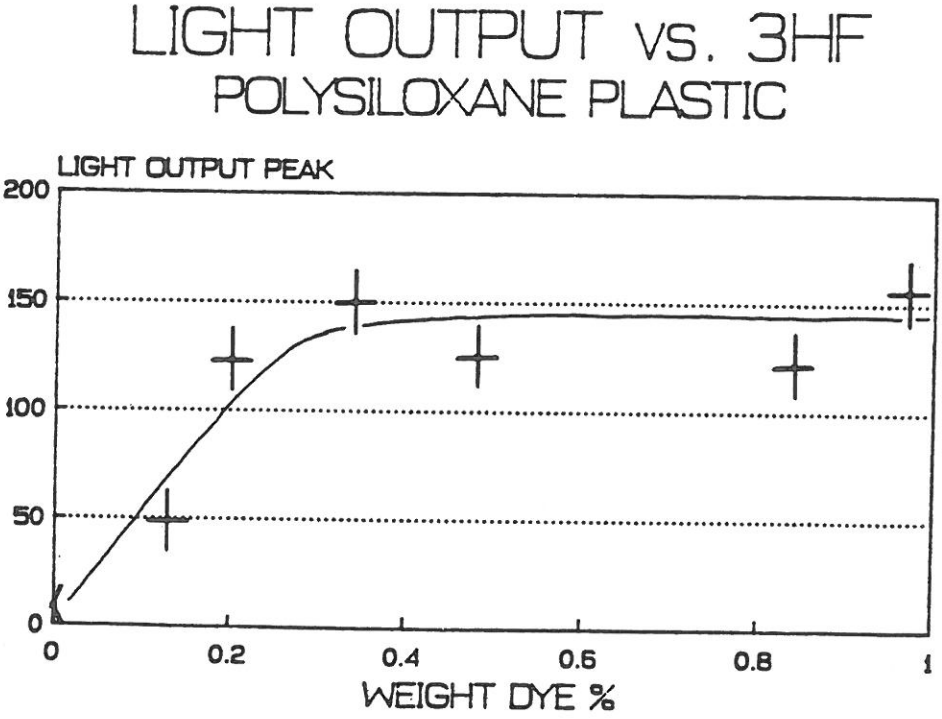
LIGHT OUTPUT vs. 3HF
POLYSILOXANE PLASTIC
LIGHT OUTPUT PEAK
200
150
100
50
0
0
0.2
0.4
0.6
0.8
1
WEIGHT DYE %

FIGURE 3

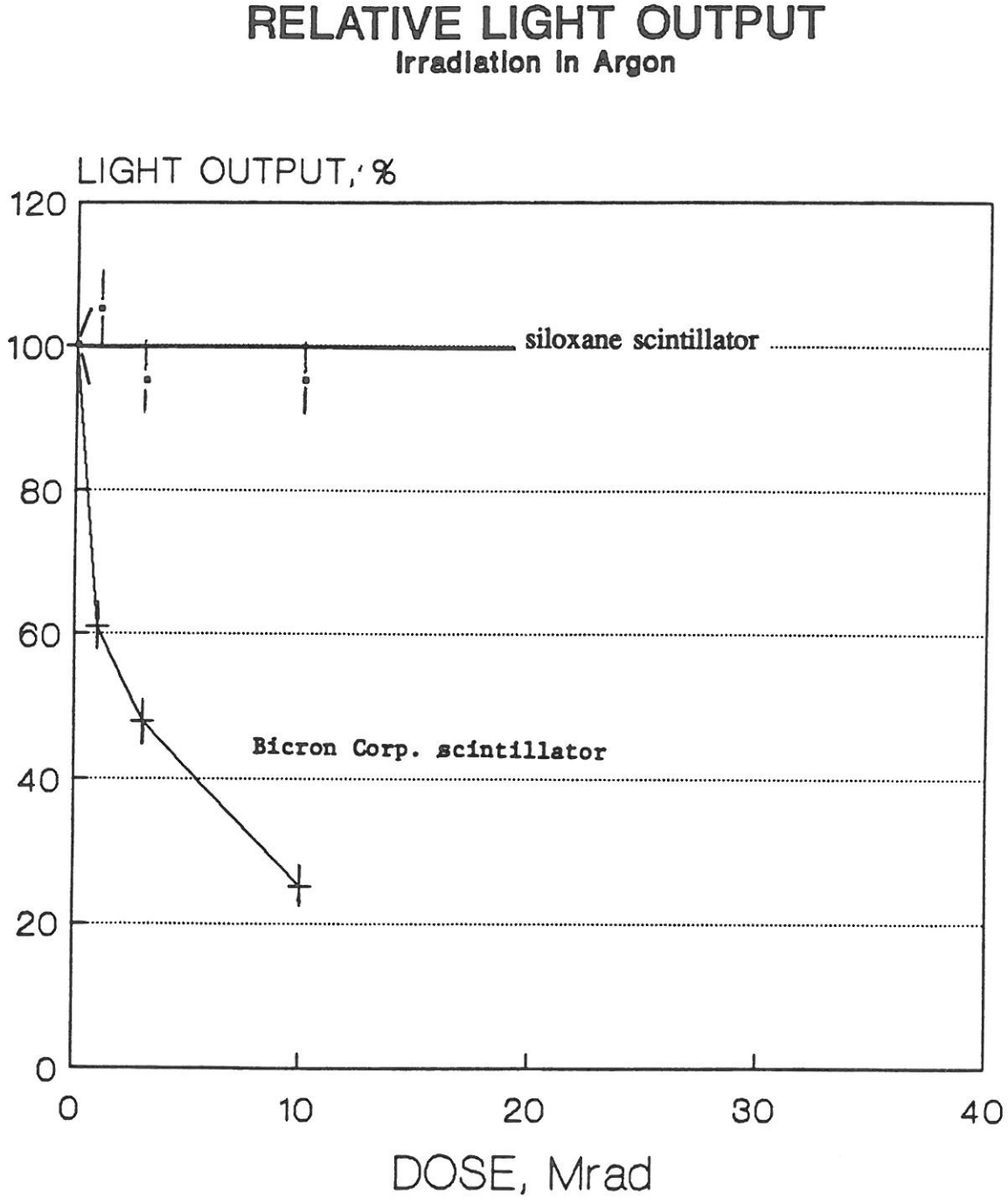
RELATIVE LIGHT OUTPUT
Irradiation in Argon
LIGHT OUTPUT, %
120
100
80
60
40
20
0
siloxane scintillator
Bicron Corp. scintillator
0
10
20
30
40
DOSE, Mrad

FIGURE 4

Ionizing Radiation Environment in SSC Detectors *

Donald E. Groom†

Lawrence Berkeley Laboratory 50-308, Berkeley CA 94720

Estimates of ionizing dose and neutron fluence have been made for typical SSC detector configurations exposed to radiation from p-p collisions. Ionizing dose from direct particle flux from the interaction point depends only upon the inverse square of the distance from the beam line. Using a description of "average events" in conjunction with simulations of secondary processes, it is found for calorimetry that the ionizing dose rate can be adequately expressed as

$$\dot{D} = \frac{A}{r^2 \sin^{2+\alpha}\theta} \ .$$

Here A depends on the process and exposure time, α is slightly less than unity, and r is the distance from the interaction point. Under nominal operating conditions, an calorimeter element 2 m from interaction point and 6° from the beam line is subjected to an annual dose of 30 kGy at electromagnetic shower maximum.

This report includes provisional correction of an error in electromagnetic dose discovered in the Task Force Report.‡

1. Introduction

An SSC Central Design Group task force was formed to assess radiation levels to be expected in SSC detectors. Its findings are available in a thick report[1], and short versions have also been published[2]. Radiation *effects* were addressed by a separate task force[3]. In this report we present a very brief discussion of radiation levels.

This particular report is for a workshop on radiation damage to plastic scintillator. According to current wisdom[6], primary neutron damage to such materials in the environment of high-energy hadron colliders is totally insignificant as compared with the effects of ionizing radiation. *Secondary* effects exist, of course, because neutron recoil products are often ionizing. To the best of our knowledge such effects are relatively minor and are readily explained. Accordingly, all discussion of the neutron flux is omitted from this report.

---

* This report is based on a version published in the *Proceedings of the ECFA Conference on Future Accelerators,* Madrid, Spain (Sept. 1989), but differs from it in three important respects: Table 1 in that report was wrong, and has now been corrected, the electromagnetic dose has been corrected (see the footnote below), and two figures specific to the detector being proposed by the Solenoid Detector Collaboration have been added.

† For the SSC Central Design Group Task Force on Radiation Levels in the SSC Interaction Regions: F. S. Alsmiller, R. G. Alsmiller, Jr., S. Ban, J. E. Brau, K. W. Edwards, A. Fassò, H. Fesefeldt, T. A. Gabriel , M. G. D. Gilchriese (Chairman), D. E. Groom, H. Hirayama, H. Kowalski, H.W. Kraner, N. V. Mokhov, D. R. Nygren, F. E. Paige, J. Ranft, J. S. Russ, H. Schönbacher, T. Stanev, G. R. Stevenson, A. Van Ginneken, E. M. Wang, R. Wigmans, and T. P. Wilcox, Jr.

‡ The maximum dose in the electromagnetic calorimeter due to incident photons from primary π^0 decay, as reported in Ref. 1 and in numerous conference proceedings, was high by a factor of three because of a trivial conversion error in Appendix 7. Corrected results given here. They are thought to be correct for the metallic part of the calorimeter, but to obtain the dose in the active part of the calorimeter they should probably be corrected upward by the stopping power ratio for the two media. For lead/scintillator the ratio is about 1.6.

This assessment could be wrong, and with some low priority neutron irradiations should be carried out. However, in most experimental test situations we can imagine, damage by boiloff neutrons (with the $\approx$ 1 MeV spectrum expected in the SSC environment) is completely overwhelmed by damage by incidental gamma rays. Reactor sources also produce a copious thermal neutron flux not present at accelerators. It is our subjective conclusion that experiments in which effects of the several kinds of irradiation are not unraveled are of very limited usefulness.

2. Assumptions

On the basis of SSC design parameters and extrapolation from S$\bar{\text{p}}$pS and Tevatron operating experience, the following assumptions were made:

- The machine luminosity at $\sqrt{s} = 40$ TeV is $\mathcal{L} = 10^{33}\,\text{cm}^{-2}\text{s}^{-1}$, and the p-p inelastic cross section is $\sigma_{\text{inel}} = 100$ mb. This luminosity is effectively achieved for 10^7 s yr^{-1}. The interaction rate is thus 10^8 s^{-1}, or 10^{15} yr^{-1}.
- All radiation comes from p-p collisions at the interaction point. For the SSC, the nominal luminosity contributes (300 hr)$^{-1}$ to the reciprocal current lifetime, so p-p collisions contribute as much radiation as dumping one of the beams into the apparatus every 6 days. Moreover, any process of comparable importance would prevent normal operation of the machine.
- The charged particle distribution is (a) flat in pseudorapidity for $|\eta| < 6$ and (b) has a momentum distribution whose perpendicular component is independent of rapidity, or approximately independent of pseudorapidity:

$$\frac{d^2N_{\text{ch}}}{d\eta dp_\perp} = H\, f(p_\perp) \tag{1}$$

  (where $p_\perp = p\sin\theta$). Integrals involving $f(p_\perp)$ are simplified by replacing $f(p_\perp)$ by $\delta(p_\perp - \langle p_\perp\rangle)$; in the worst case this approximation introduces an 8% error.
- Gamma rays from π^0 decay are as abundant as charged particles. They have approximately the same η distribution, but half the mean momentum.
- The values $H \approx 7.5$ and $\langle p_\perp\rangle \approx 0.6$ GeV/c for $\sqrt{s} = 40$ TeV are obtained by extrapolating experimental results[4, 5], and are in good agreement with results obtained with standard fragmentation models. These values together with Eq. (1) are thought to describe particle production at the SSC within a factor of two or better.

3. Dose from direct particle production

Since $d\eta/d\Omega = (2\pi\sin^2\theta)^{-1}$, it follows from Eq. (1) that the flux of charged particles from the interaction point passing through a normal area da located a distance $r_\perp$ from the beam line is given by

$$\frac{dN_{\text{ch}}}{da} = \frac{1.2\times 10^8\,\text{s}^{-1}}{r_\perp^2}\,. \tag{2}$$

In a typical organic material, a relativistic charged particle flux of 3×10^9 cm^{-2} produces an ionizing radiation dose of 1 Gy, where 1 Gy $\equiv$ 1 joule kg^{-1} (= 100 rads). The above result may then be rewritten as

$$\dot{D} = \frac{0.4 \text{ MGy yr}^{-1}}{r_\perp^2} \tag{3}$$

for an absorber much thinner than a nuclear interaction length, where $r_\perp$ is in cm.

In the presence of a magnetic field, low-energy particles make multiple passes through a test sample and so contribute to the dose more than once. This increases dose by about a factor of two.

Further dose enhancements might be expected from the secondary radiation ("albedo") of objects subjected to very high incident flux. For example, tracking devices which can "see" small-angle parts of the calorimetry will be subjected to back-scattered ionizing radiation.

4. Dose and fluence in a calorimeter

In a medium in which cascades can develop, the ionizing dose or neutron flux is at least roughly proportional to the particle energy striking unit area at a distance r from the interaction point. The charged particle flux is proportional to $(r^2 \sin^2\theta)^{-1}$, and the energy carried by the particles is proportional to $\langle E \rangle \approx p = p_\perp / \sin\theta$. The dose or fluence at cascade maximum is hence proportional to $1/(r^2 \sin^3\theta)$. Symbolically, this logic flow is as follows:

$$\left.\begin{aligned} \frac{dN_{\text{ch}}}{d\eta} &= \text{Const} \\ \frac{d\eta}{d\Omega} &= \frac{1}{2\pi \sin^2\theta} \end{aligned}\right\} \frac{dN_{\text{ch}}}{d\Omega} = \frac{\text{Const}}{\sin^2\theta} \left.\begin{aligned} & \\ E \approx p &= \frac{p_\perp}{\sin\theta} \end{aligned}\right\} \frac{dE}{d\Omega} = \frac{\text{Const}}{\sin^3\theta} \left.\begin{aligned} & \\ & \\ \frac{d\Omega}{da} &\propto \frac{1}{r^2} \end{aligned}\right\} \begin{matrix} \text{Neutron fluence} \\ \text{or ionizing dose} \end{matrix} = \frac{K}{r^2 \sin^3\theta} \tag{4}$$

This result is incomplete for a number of reasons. In the first place, the constant K must come from Monte Carlo simulations, hopefully supplemented by experimental measurements. Secondly, since showers lengthen with energy the maximum amplitude is not quite proportional to the incident energy density, so that the power of $\sin\theta$ is a little less than three. This is true for both electromagnetic and hadronic cascades. Finally, hadronic activity increases less rapidly than linearly with energy because π^0 production progressively "bleeds off" more and more energy to the electromagnetic channel as the incident energy increases, further reducing the power of $\sin\theta$ for processes such as neutron production. Even in this case, the combined effect is to reduce the exponent to about

2.7, so the above equation still provides guidance. The inverse r^2 dependence remains rigorously true, providing a serious constraint on detector design.

We rewrite the result as

$$\text{Ionizing dose rate} \equiv \dot{D} = \sigma_{\text{inel}} \int \mathcal{L} dt \, \frac{H \langle p_\perp \rangle^\alpha}{r^2} \frac{\text{Constant}}{\sin^{2+\alpha} \theta} = \frac{A}{r^2} \cosh^{2+\alpha} \eta \tag{5}$$

where the dependence on some machine-dependent parameters is made explicit. The second form is obtained with the aid of the identity $\cosh \eta = \sin \theta$.

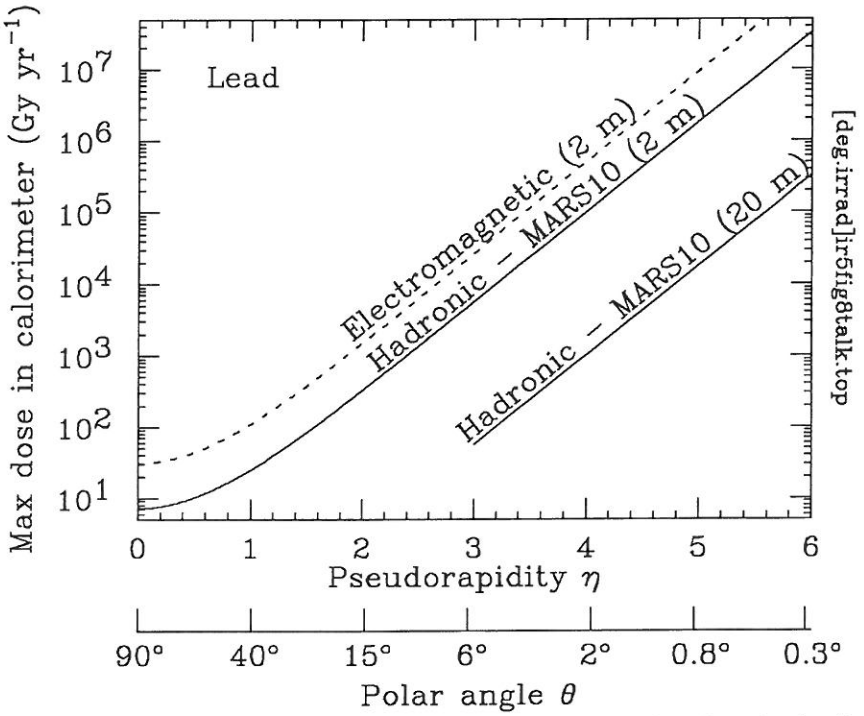

FIG. 1. The maximum hadronic dose as a function of pseudorapidity for a lead sphere, assuming that the maximum dose occurs at the indicated radius. The maximum electromagnetic dose in 1:1 uranium:scintillator is shown by the dashed line. Since the radiation length, nuclear interaction length, and density are nearly identical for the two materials, dose (but not neutron flux) results may be compared directly. The electromagnetic dose has been corrected downward by a factor of three, as described in an earlier footnote. Doses are for the high-Z absorber in the calorimeter, and should probably be corrected upward by a stopping power ratio (1.4 for silicon and 1.6 for scintillator) to obtain the dose in the sensitive material.

Values of A and α are given in Table 1 for the maximum dose rate produced by hadrons and photons from the interaction point. The corresponding functions (Eq. 5) are shown in Fig. 1. The electromagnetic maximum dose under standard conditions ($\mathcal{L} = 10^{33}\,\text{cm}^{-2}\text{s}^{-1}$, 1 yr $\equiv 10^7$ s) and high-luminosity conditions ($\mathcal{L} = 10^{34}\,\text{cm}^{-2}\text{s}^{-1}$, 10 yr $\equiv 10^8$ s) is shown in Figs. 2 and 3.

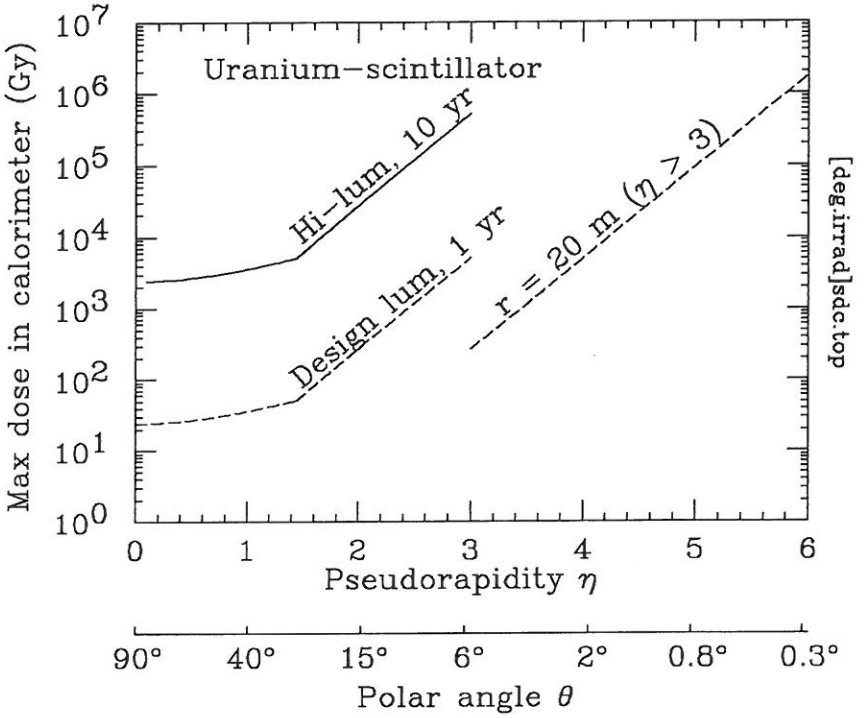

FIG. 2. The maximum dose from incident photons shown in Fig. 1, scaled to the dimensions of the SDC calorimeter (2.2 m to shower maximum in the radial direction, 4.7 m in the z direction). The dotted lines are for standard luminosity for one year, and the solid line is for $\mathcal{L} = 10^{34}\,\mathrm{cm}^{-2}\mathrm{s}^{-1}$ for 10 years.The doses have been corrected downward by a factor of three from those given in Ref. 1, as described in an earlier footnote.

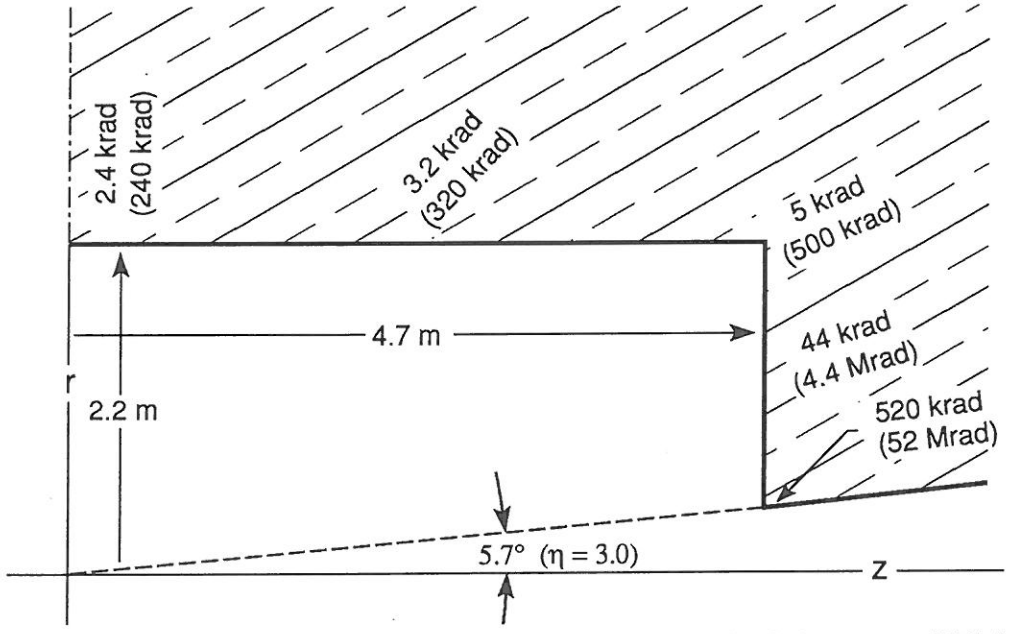

FIG. 3. Ionizing dose at electromagnetic shower maximum in the SDC detector at SSC design luminosity for one year and (in parenthesis) at $\mathcal{L} = 10^{34}\,\mathrm{cm}^{-2}\mathrm{s}^{-1}$ for 10 years. The doses have been corrected downward by a factor of three from those given in Ref. 1, as described in an earlier footnote, and are for the high-Z absorber, not the sensitive material.

Table 1

Coefficients $A/(100\ \mathrm{cm})^2$ and α for the evaluation of radiation levels at cascade maximum in SSC calorimetry under nominal operating conditions. At a distance r and angle θ from the interaction point the annual fluence or dose is $A/(r^2 \sin^{2+\alpha}\theta)$.

Quantity	$A/(100\ \mathrm{cm})^2$	Units	$\langle p_\perp \rangle$	α
Dose rate from photons	124*	Gy yr^{-1}	0.3 GeV/c	0.93
Dose rate from hadrons	29	Gy yr^{-1}	0.6 GeV/c	0.89

*Corrected value.

On the average, a certain fraction of an electromagnetic shower at a given energy is contained in a distance $n_{EM}X_0$, where X_0 is a radiation length in the material. Similarly, a hadronic shower is contained in a distance $n_{\mathrm{had}}\lambda_I$, where λ_I is the nuclear interaction length. Very roughly, $n_{EM} \approx 20$ and $n_{\mathrm{had}} \approx 6$ for 99% containment at 1 GeV. About half as much energy is carried by π^0's as by other hadrons. We thus expect the maximum dose due to photons from π^0 decay to be about $\frac{1}{2}(n_{\mathrm{had}}\lambda_I)/(n_{EM}X_0)$ times the dose at hadronic cascade maximum. The radiation length in lead is 6.37 g cm^{-2}, and the nuclear interaction length is 194 g cm^{-2}. The ratio is about 5, while the ratio obtained from Table 1 is 9.1. The agreement is regarded as satisfactory, given the uncertainty in n_{had} and n_{EM}.

6. Scaling to other machines

Using the scaling discussed in connection with Eq. (5) above, examples of scaling to other accelerators are given in Table 2. It should be noted that the assumption that all radiation comes from the interaction point does not apply to the present generation of accelerators.

Table 2

A rough comparison of beam-collision induced radiation levels in calorimetry at the Tevatron, УНК, high-luminosity LHC, and SSC.

	Tevatron	УНК-3	LHC	SSC
$\sqrt{s}$ (TeV)	1.8	6	16	40
$\mathcal{L}_{\mathrm{nom}}$ ($\mathrm{cm}^{-2}\mathrm{s}^{-1}$)	2×10^{30}	4×10^{32}	4×10^{34}†	1×10^{33}
σ_{inel}	59 mb	80 mb	86 mb	100 mb
H	4.1	4.5	6.3	7.5
$\langle p_\perp \rangle$ (GeV/c)	0.46	0.52	0.55	0.60
Scale factor‡	5×10^{-4}	0.2	27	1

† High-luminosity option.

‡ Proportional to $\mathcal{L}_{\mathrm{nom}}\,\sigma_{\mathrm{inel}}\,H\,\langle p_\perp \rangle^{0.7}$

7. References

1. "Report of the Task Force on Radiation Levels in the SSC Interaction Regions," ed. by D. E. Groom, SSC Central Design Group Report SSC-SR-1033 (June 1988).
2. D. E. Groom, Nucl. Instrum. Methods **A279**, 1 (1989);
   D. E. Groom, pp. 711–716 in *Proc. of the 1988 Summer Study on High Energy Physics in the 1990's,* Snowmass CO, June 27–July 15, 1988, ed. S. Jensen, World Scientific (1989);
   D. E. Groom, *Proc. of the Workshop on Calorimetry for the Superconducting Super Collider,* Tuscaloosa, Alabama, 13–17 March 1989, ed. by R. Donaldson and M. G. D. Gilchriese, World Scientific (to be published, June 1990).
3. "Radiation Effects at the SSC," ed. by M. G. D. Gilchriese, SSC Central Design Group Report SSC-SR-1035 (June 1988).
4. F. Abe *et al.* (CDF), Phys. Rev. Lett. **61**, 1819 (1988).
5. G. J. Alner *et al.* (UA5), Z. Phys. C **33**, 1-6 (1986).
6. H. Schönbacher and R. Clough, private communications (1990).

ELECTROMAGNETIC SHOWERS RESOLUTION IN A SCINTILLATING FIBERS CALORIMETER

J.Badier
Ecole Polytechnique , LPNHE
Palaiseau , F - 91128

ABSTRACT

Some effects of radiation damage on a scintillating plastic fiber calorimeter are presented. The study is limited to the non linearity and to the resolution degradation in electron energy measurements. The influences of light emission loss and of the increase in attenuation length have been independently taken into account. We conclude that at LHC, with presently available fibers, the precision of measured energy for electrons may be kept within 1% over ten years for polar angles greater than 20 ^{0} measured from the beam axis. Between 10 ^{0} and 20 ^{0} the fiber quality must be improved to yield the same precision.

1. Introduction

The electrons identification and measurement are a basic necessity in the design feature of a LHC detector. The scintillating fiber calorimetry is an attractive solution. Its main risk consists in the radiation damage effects. The light yield is sufficient to permit a loss without any sampling erosion; an overall suitable calibration is assumed to correct the raw datas; unfortunately the non linearity with the energy and the resolution damaging cannot be corrected in any case. The electromagnetic part of the calorimeter concerns the 20 first radiation lengths, that is 15 cm over a 200 cm total length. This region is loaded by the large radiation dose coming from the primary π^0s decaying into gammas pairs. We will use a simple parametrisation of the electromagnetic showers to study the radiation damage.
The following notation will be used :

x , X : Calorimeter depths in radiation lengths
z , Z : Calorimeter depths in cm
e , E : Energies in Gev
s , S : Scintillator emitted light.
q , Q : Transmitted light to the photomultiplier.

2. Showers parametrisation

The electromagnetic part of the calorimeter is essentially irradiated by π^0s. An additional flat background is induced by the charged hadrons. A good parametrisation allows to make simple calculations without handling of big packages like EGS. The mean longitudinal distribution of an electronic shower can be parametrised [1] by the formula :

$$dN/dx = B^A x^{A-1} \exp(-Bx) / \Gamma(A) \qquad (1)$$

The mean value m and the r.m.s. σ of this distribution are related to A and B :

$$m = A / B \qquad (2)$$
$$\sigma^2 = A / B^2 \qquad (3)$$

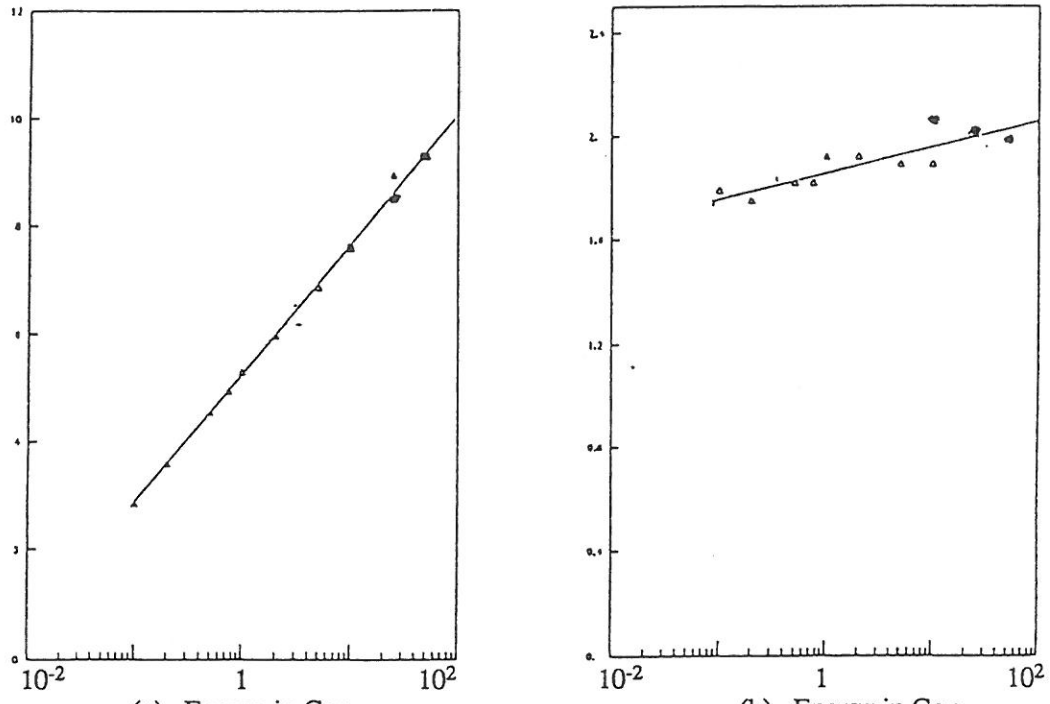

(a) Energy in Gev (b) Energy in Gev

Figure 1. Variation of the mean shower parameters with energy. The full dots are from measurements, the open triangles from EGS. (a) Mean value m, (b) σ^2 / m .

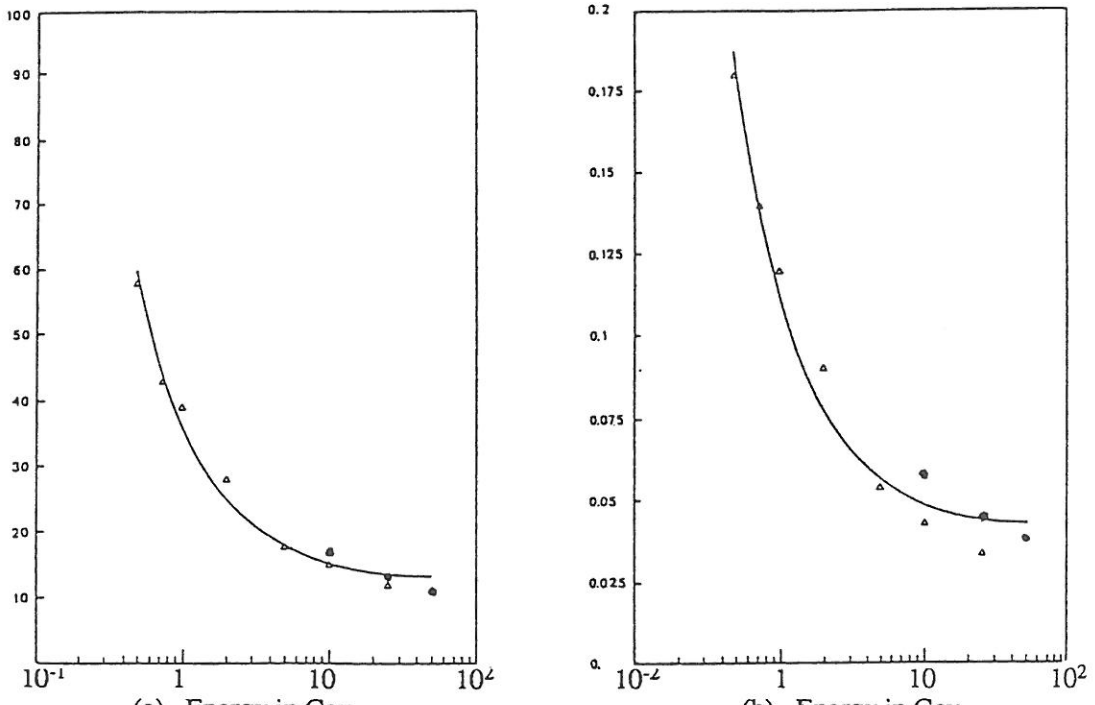

(a) Energy in Gev (b) Energy in Gev

Figure 2. Deviation of the shape parameters as a function of energy. The full dots are from measurements, the open triangles from EGS. (a) $[d(1/m)/(1/m)]^2$, (b) $[d(\sigma^2/m^2)/(\sigma^2/m^2)]^2$.

Generally A is expressed as a linear form of ln(E), B been taken constant. It is preferable to parametrise m and σ^2/m to have a larger validity range (fig.1a)[2]. Numerically , in radiation lengths units :

$$m = 5.37 + 1.04 \ln(E) \quad (4)$$
$$\sigma^2 / m = 1.86 + 0.04 \ln(E) \quad (5)$$

Individual cascades have fluctuations larger than the sampling ones above 1 Gev. It is an experimental observation than 1/m and σ^2 / m^2 are uncorrelated and gaussianlike with relative r.m.s. parametrised in following way (fig.1b)[2]:

$$[d(1/m)/(1/m)]^2 = 0.013 + 0.021 / E \quad (6)$$
$$[d(\sigma^2/m^2)/(\sigma^2/m^2)]^2 = 0.041 + 0.066 / E \quad (7)$$

The numerical values of the coefficients were obtained using a Pb/Al (4::3) calorimeter [3] and correcting them for a Pb/Scintillator medium by a scaling of the energy with the energy loss per radiation length.

Table I. Mean medium properties.

Material	Density ρ	Radiation length	Energy loss	Energy loss per rad. l.
	g/cm^3	g/cm^2	$Mevcm^2/g$	Mev
Pb/Al(4::3)	7.64	7.66	1.24	9.50
Pb/Sc(4::1)	9.29	6.49	1.32	8.57

3. Dose rate estimation

The impulsion P of the emitted π^0s have an exponential behaviour :

$$dN / dP = \exp(- P / \langle P \rangle) \quad (8)$$

Generating such π_0s and applying the parametrisation to the final electrons and positrons one obtains the deposited energy distribution. The coordinates of the maximum of 1/E.dE/dx may be parametrised :

$$x_{max} = 4.08 + 1.16 \ln(\langle P \rangle) \quad (9)$$
$$1/E.dE/dx|_{max} = .137 - .025 \ln(\langle P \rangle) \quad (10)$$
$$z_{max} = 2.85 + 0.81 \ln(\langle P \rangle) \quad (11)$$
$$1/E.dE/dz|_{max} = .196 - .036 \ln(\langle P \rangle) \quad (12)$$

The number of emitted π^0s per steradians and per year, with the polar angle θ [4] leads to the expressions of the dose profile and of its integral :

$$dN / d\Omega = L_{um}\, t\, \sigma_{tot}\, (dn/d\eta) / 2\pi \sin^2\theta \quad (13)$$
$$Dose(z) = 1.6\ 10^{-5}\ (dN / d\Omega) \langle P \rangle\ (1/E.dE/\rho dz) / (R+z)^2 \text{ Rad} \quad (14)$$
$$\text{Integrated dose} = 1.6\ 10^{-5}\ (dN / d\Omega) < P > / \rho R^2 \text{ Rad cm} \quad (15)$$

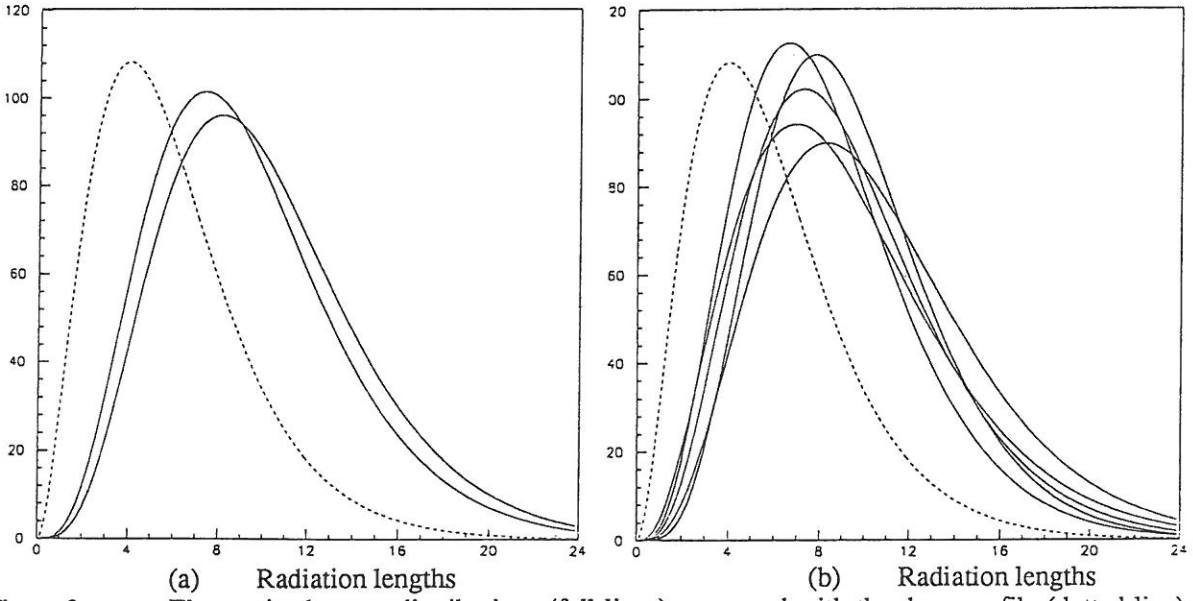

Figure 3. Electronic showers distributions (full lines) compared with the dose profile (dotted line) induced by .6 Gev π^0s. (a) Mean shape of 50 Gev and 100 Gev electronic showers. (b) Shape fluctuations of 50 Gev showers.

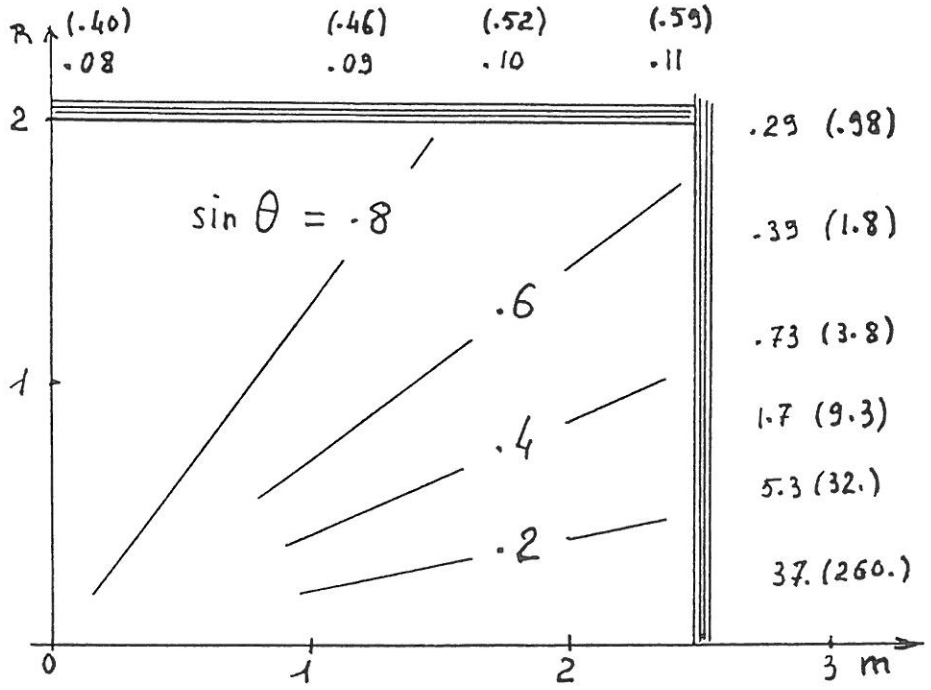

Figure 4. Maximum dose per year in a typical calorimeter at LHC. θ is the polar angle with respect to the beam. Doses are expressed in Mrad. The quantities between brackets are the integrated doses expressed in Mrad cm.

The figure 3 gives some electrons showers profiles compared to the dose profile induced by .6 Gev π^0s. The variation of the mean shape with the electron energy is responsible of the non linearity, the fluctuations at a fixed energy are responsible of the resolution loss.

At LHC, the luminosity $L_{um} = 4.10^{34}$ cm^{-2} sec^{-1} , during a time $t = 10^7$ sec per year. At the energy of 16 Tev, the total cross section is $\sigma_{tot} = 85$ mb , the mean momentum of the π^0s is $<P> = .6 / \sin\theta$ Gev/c and their number per interaction and rapidity interval is $dn/d\eta = 3$. One finds $dN / d\Omega = 1.6\ 10^{16} / \sin^2\theta$.
The repartition of the maximum dose in a typical calorimeter is sketched in figure 4.

4. Emission loss of light:

Putting aside the absorption along the fiber, the irradiation of a point of the scintillator decreases the emitted light in accordance with :

$$s(z) = s_0(z) \exp\ (-\text{Dose}(z) / \gamma) \qquad (13)$$

s_0 is the light yield before irradiation, γ is the scintillator life expressed in dose units. Depending of the fiber type, γ varies from 10 to 100 Mrad .

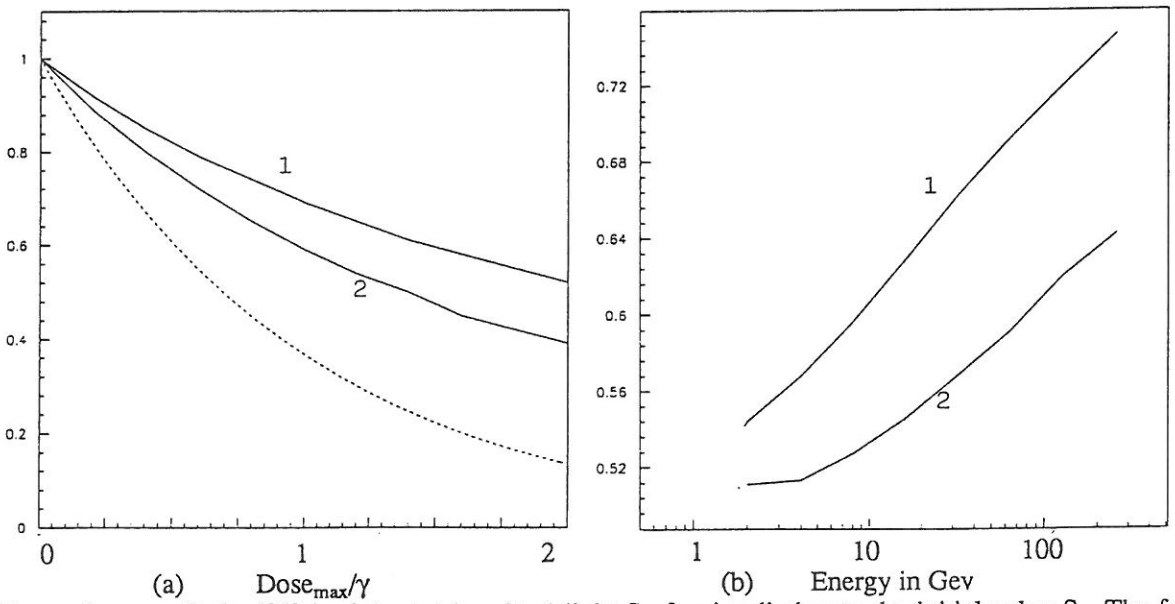

Figure 5. Ratio (S/S_0) of the total emitted light S after irradiation to the initial value S_0. The full lines 1 and 2 correspond respectively to irradiating π_0s of .6 and 2.4 Gev. (a) S/S_0 variation with Dose$_{max}$/γ for 64 Gev electrons. The dotted line gives the loss at the maximum of the dose. (b) S/S_0 variation with the electron energy for Dose$_{max}$ / γ = .5

The distribution of $s_0(z)$ along the unirradiated fiber is proportional to the shower energy profile. The total emitted light S after irradiation is obtained by integrating s(z) over z. The dose distribution depends of the mean momentum <P> and of the flux of the primary π_0s. The ratio of the maximum dose to γ is a convenient way to characterize this distribution.

The dependance of S with the radiation level is displayed in figure 5a. The non linearity with the incident electron energy appears in figure 5b, in order to express it numerically, one uses the quantity $\delta = [\ S(E) - 2\ S(E/2)\ ] / S(E)$ which is the relative difference between an asymetric and a symetric electron pair coming from a gamma materialisation. The dependance of δ with <P> and E is small.

$$\delta = .044\ Dose_{max} / \gamma \qquad (14)$$

$\delta = 1\%$ corresponds to $Dose_{max} / \gamma = .23$
Similarly the resolution degradation $\Delta E/E$ due to the showers fluctuations is rather constant.
With <P> = .6 Gev and E = 100 Gev one has :

$$\Delta E/E = .068\ Dose_{max} / \gamma \qquad (15)$$

$\Delta E/E = 1\%$ corresponds to $Dose_{max} / \gamma = .15$

A fiber with a coefficient $\gamma = 100$ Mrad withstands a radiation level of 20 Mrad.

5. Uniform absorption.

The absorption coefficient K_0 of a non irradiated fiber is the inverse of its attenuation length. An uniform radiation dose increases this coefficient. The distance to the photomultiplier is such that the transmission by the cladding has not to be taken in account. Calling L the fiber length and r the reflection of the mirror at the fiber entrance, the attenuation of the transmitted light q is :

$$q/q_0 = e^{-KL} (e^{-Kz} + r\ e^{Kz}) \qquad (16)$$

One may develop the exponentials , Kz being small :

$$q = q_0\ e^{-KL}\ (1+r)\ (\ 1 + Kz(1-r)/(1+r) + K^2z^2/2\ ) \qquad (17)$$

$q_0(z)$ is the electronic shower profile. The integrations over z from 0 to L of $q_0(z)$, $zq_0(z)$ and $z^2q_0(z)$ are respectively equal to Q_0 , mQ_0 and $(m^2+\sigma^2)\ Q_0$. m and σ are the mean value and the r.m.s. expressed in cm and deduced from (2),(3). The total transmitted light Q is :

$$Q = Q_0\ e^{-KL}\ (1+r)\ (1 + Km(1-r)/(1+r) + K^2(m^2+ \sigma^2)/2\ ) \qquad (18)$$

Aside the mean lost $e^{-KL}(1+r)$ the dependance of m and σ with the energy induces a non linearity. Defining it again as $\delta = [\ Q(E) - 2\ Q(E/2)\ ] / Q(E)$ one finds :

$$\delta = .50\ K(1-r)/(1+r) + (2.13 + .38\ \ln(E)\ )\ K^2 \qquad (19)$$

To have $\delta < 1\%$ at an energy of 100 Gev, one needs :

$1/K > 20$ cm with $r = 1$
$1/K > 50$ cm with $r = 0$

By derivation of the formula (18) with respect to m and σ/m and using the parameters given in (6) and (7) one obtains the error $\Delta E/E$ from the showers fluctuations. It is weakly energy dependent. For E = 100 Gev,one has :

$\Delta E/E = 1.5\ K^2$ with $r = 1$
$\Delta E/E = .8\ K$ with $r = 0$

The errors due to the increased attenuation lengthes are small and it is sufficient to consider the mean loss effect (e^{-KL}).

6. Localised absorption.

At the entrance of the fiber, the dose repartition is not uniform, leading to an absorption $K(z) = K_0 + \alpha Dose(z)$. Calling Σ_{Dose} the integrated dose (15) and using a δ distribution approximation , one has :

$$K(z) = K_0 + \alpha\Sigma_{Dose}\ \delta(z-Z) \tag{20}$$

One chooses Z as the maximum irradiation abcissa. The α coefficient characterises the radiation hardness of the fiber. Depending of the fiber type and of the recuperation conditions , α varies from 10^{-2} to 10^{-3} $cm^{-1}Mrad^{-1}$. The formula (20) leads to a transmission factor $T = \exp(-\alpha\Sigma_{Dose})$ localised at the abcissa Z. One forgets the K_0 term which was studied in the precedent paragraph.
To calculate the light q(z) on the photomultiplier, two cases have to be considered, depending of the abcissa z of the emitted light with respect to Z.

If $z < Z$, $q(z) = s_0(z)\ (\ T + Tr\ )$.
If $z > Z$, $q(z) = s_0(z)\ (\ 1 + T^2r\ )$.

$s_0(z)$ is the emitted light yield precedently used in (13). It varies like the electronic shower profile and one assumes that it is normalised to the energy. The integral of s_0 from 0 to L is E , and from 0 to Z is EF_0. The total light arriving to the photomultiplier is Q :

$$Q/E = F_0(T+Tr) + (1-F_0)(1+T^2r) \tag{21}$$
$$Q/E = 1 + T^2r - F_0(1-T)(1-Tr) \tag{22}$$

The non linearity estimator is :

$$\delta = [F_0(E) - F_0(E/2)]\ (1-T)(1-Tr) \tag{23}$$

The shower fluctuation error is :

$$\Delta E/E = \Delta F_0(1-T)(1-Tr)/(1+r) \tag{24}$$

The quantities $F_0(E) - F_0(E/2)$ and ΔF_0 are plotted in the figure 6 with the energy E = 100 Gev. Their maximum values are respectively 10% and 6%. The true value is smaller and depends of the dose distribution.
$(1-T)(1-Tr) < .2$ insures good linearity and resolutions. Assuming a fiber with $\alpha = 10^{-3}$ $cm^{-1}Mrad^{-1}$ one finds limits of 600 Mrad cm with $r = 1$ and of 200 Mrad cm with $r = 0$.

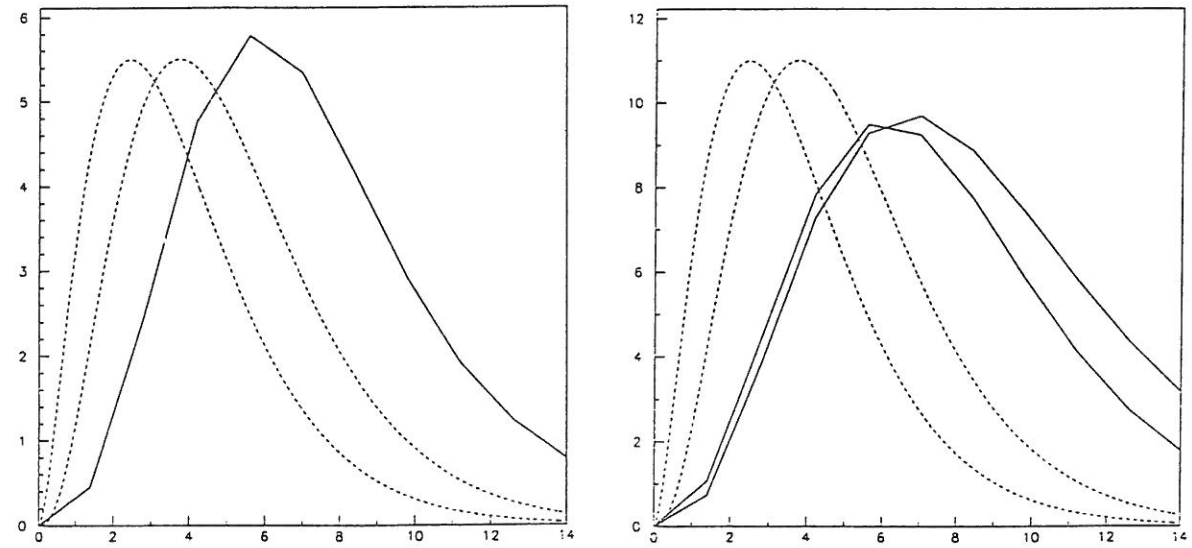

Figure 6. Quantities calculated from the integration of electronic showers.The dotted line represents the dose distribution from .6 Gev and 6. Gev π^0s.. (a)[$F_0(E) - F_0(E/2)$] in % with E = 40 Gev. (b) Fluctuations ΔF_0 in % of the integral of 20 Gev and 40 Gev showers.

6. Conclusion.

The influence of the radiation damage on the resolution and linearity in electron measurements with a scintillating fibers calorimeter has been studied, using a parametrisation of the electromagnetic showers. They agree with a precedent study [5,6].
The dose at the peak of irradiation is limited by the emission light loss. With presently available fibers it has to be smaller than 20 Mrad : one has such a level in 10 years for a polar angle of 17^0 at LHC.
The increase in the attenuation length gives a limitation to the integrated dose which has to be smaller than 600 Mrad cm assuming an entrance reflector: this condition is insured over 10 years at LHC for polar angles greater than 10^0.
It appears that the limitation due to the emission loss must not be neglected.

References.

[1] Phys. Let.,B204,66(1988)
[2] J.Badier,ALEPH 87-09,(1987)
[3] M.Bardadin,ALEPH 89-1,(1989)
[4] D.E.Groom,ECFA 89-124,103(1989)
[5] H.P.Paar,ECFA 89-124,226(1989)
[6] D.Acosta,LAA preprint,(1989)

Radiation Damage Effects on Calorimeter Compensation

Tony A. Gabriel
Oak Ridge National Laboratory
P. O. Box 2008
Oak Ridge, Tenn. 37831-6364
and
Thomas Handler
Physics Department
University of Tennessee
Knoxville, Tenn. 37996-1200

Abstract

An important consideration in the design of a detector that is to be used at the Superconducting Super Collider (SSC) is the response of the calorimeter to electromagnetic and hadronic particles and the equality of those responses for different types of particles at equal incident energies, i.e. compensation. However, as the simulations that are reported show, the compensation characteristics of a calorimeter can be seriously compromised over a relatively short period of time due to the large radiation levels that are expected in the SSC environment.

1. Introduction

As has been suggested in previous reports and at past conferences, a calorimeter to be used at the Superconducting Super Collider should have an equal response to electromagnetic and hadronic particles, if they are of the same energy. If this is the case the calorimeter is said to be compensating and the calorimeter considered in this study is of the compensating type. In order to achieve compensation, various combinations of passive and active media have been used. Plastic scintillator in combination with uranium or lead can achieve this desired result.

The detectors at the SSC will have to operate in a hostile radiation environment that has so far not been explored at previous or current accelerators. Therefore, the long term effects of exposure to radiation are unknown. However, as has been shown at this conference, plastic scintillator does experience a degradation of its output signal when exposed to the radiation doses that are equivalent to what is expected at the SSC[1]. It has also been shown that the signal output of the scintillator does not fully recover with

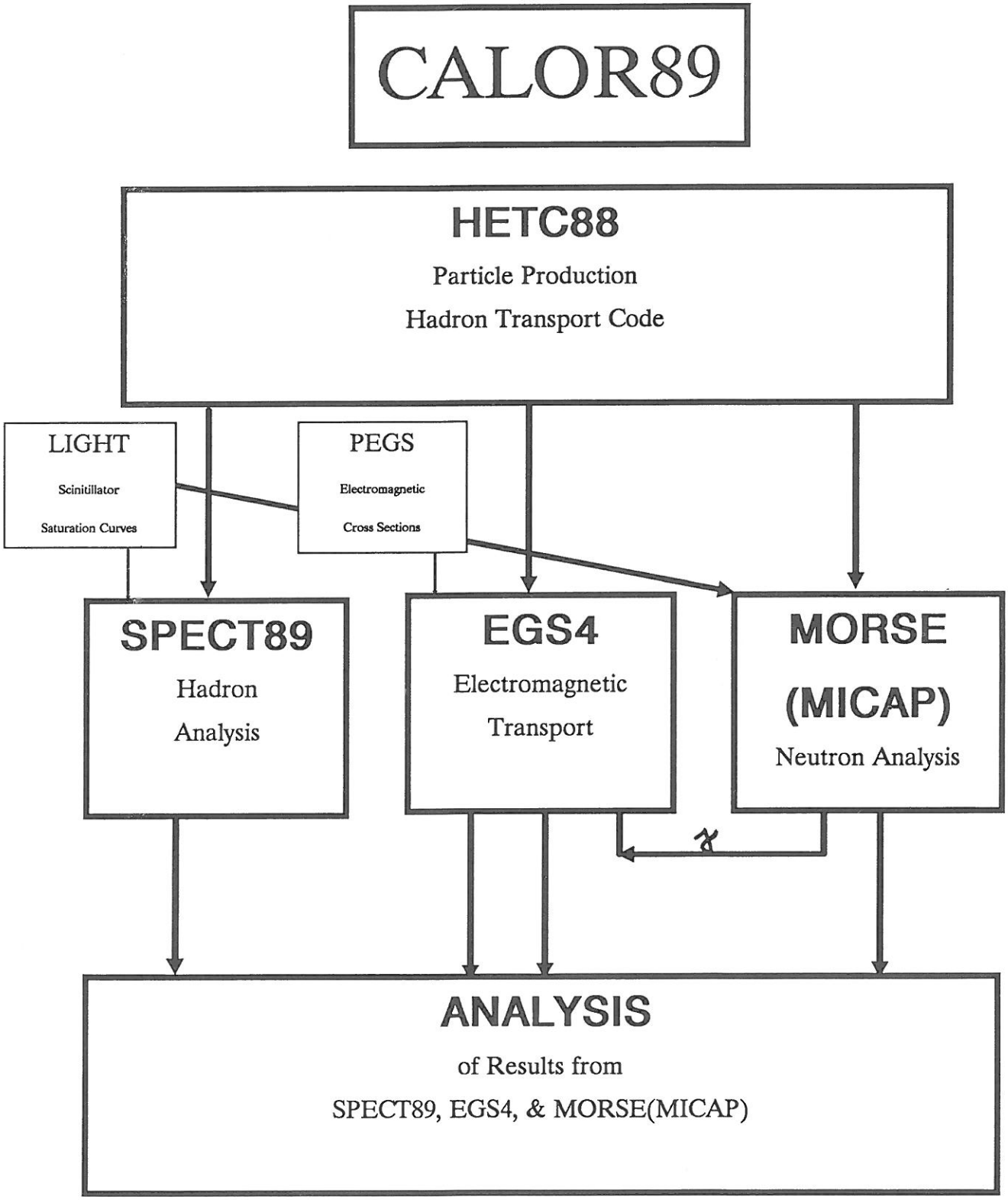

Fig. 1. The CALOR89 Code System

annealing. This implies that the response of the calorimeter will change as a function of time. To determine how the detector response will change is the object of this study.

2. Method

To determine how the response of a calorimeter changes when exposed to radiation doses expected at the SSC, a simple generic slab calorimeter has been simulated using the CALOR89 system of programs. CALOR89[2] consists (Fig. 1) of four primary programs (HETC88[3], SPECT89, EGS4[4], and MORSE[5] or MICAP[6]) plus their ancillary routines and a final analysis program. HETC88 is used to generate and transport the hadronic particles through the calorimeter, while SPECT89 does the energy deposition of the hadrons in the calorimeter. EGS4 is used for the transport and energy deposition of the electromagnetic particles in the calorimeter. MORSE or MICAP is used to transport neutrons that are below 20 MeV. The output of each of these programs (SPECT89, EGS4, MORSE or MICAP) is then used in the final analysis program.

The unit cell of the calorimeter under investigation consists of a 4mm thick lead sheet, followed by a 1mm thick sheet of plastic scintillator. The lead and plastic scintillator sheets were 2m by 2m. This unit cell is then repeated 300 times for a total calorimeter depth of 150cm. This particular configuration of active and passive media turns out to be mildly compensating with an e/h value of 1.05 in the energy range 2 - 20 GeV. To simulate the hadronic and electromagnetic particles entering the SSC calorimeter from 20 TeV p-p collisions, incident 10 GeV negative pions and electrons properly normalized are used.

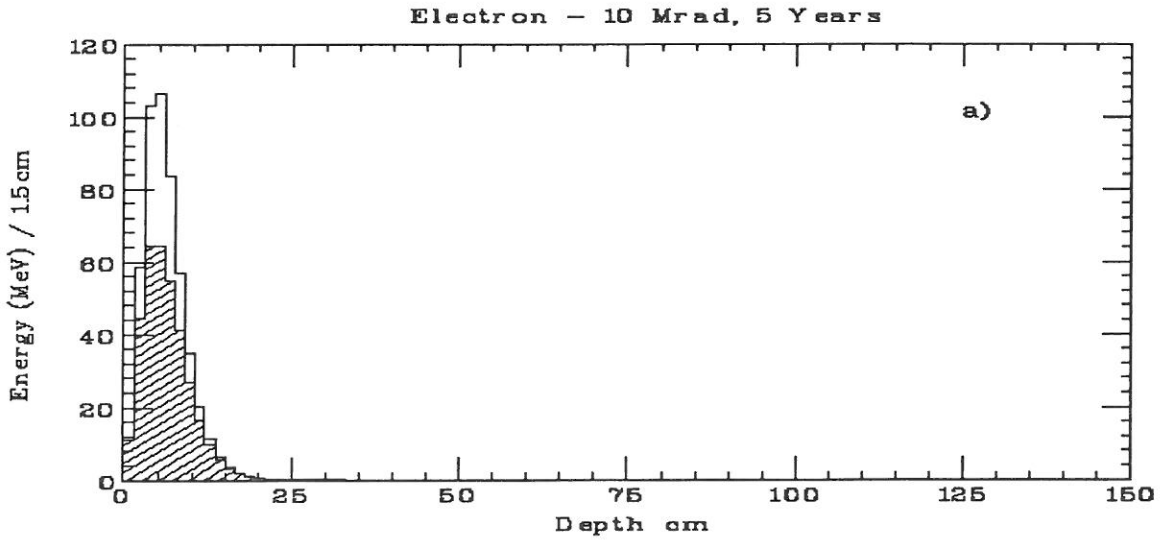

Fig 2a. Electron shower depth profile. The unshaded histogram is the original profile, while the shaded histogram is the resultant profile after 5 years at 10 Megarads/year at 1% signal loss/Megarad/year done geometrically(see text).

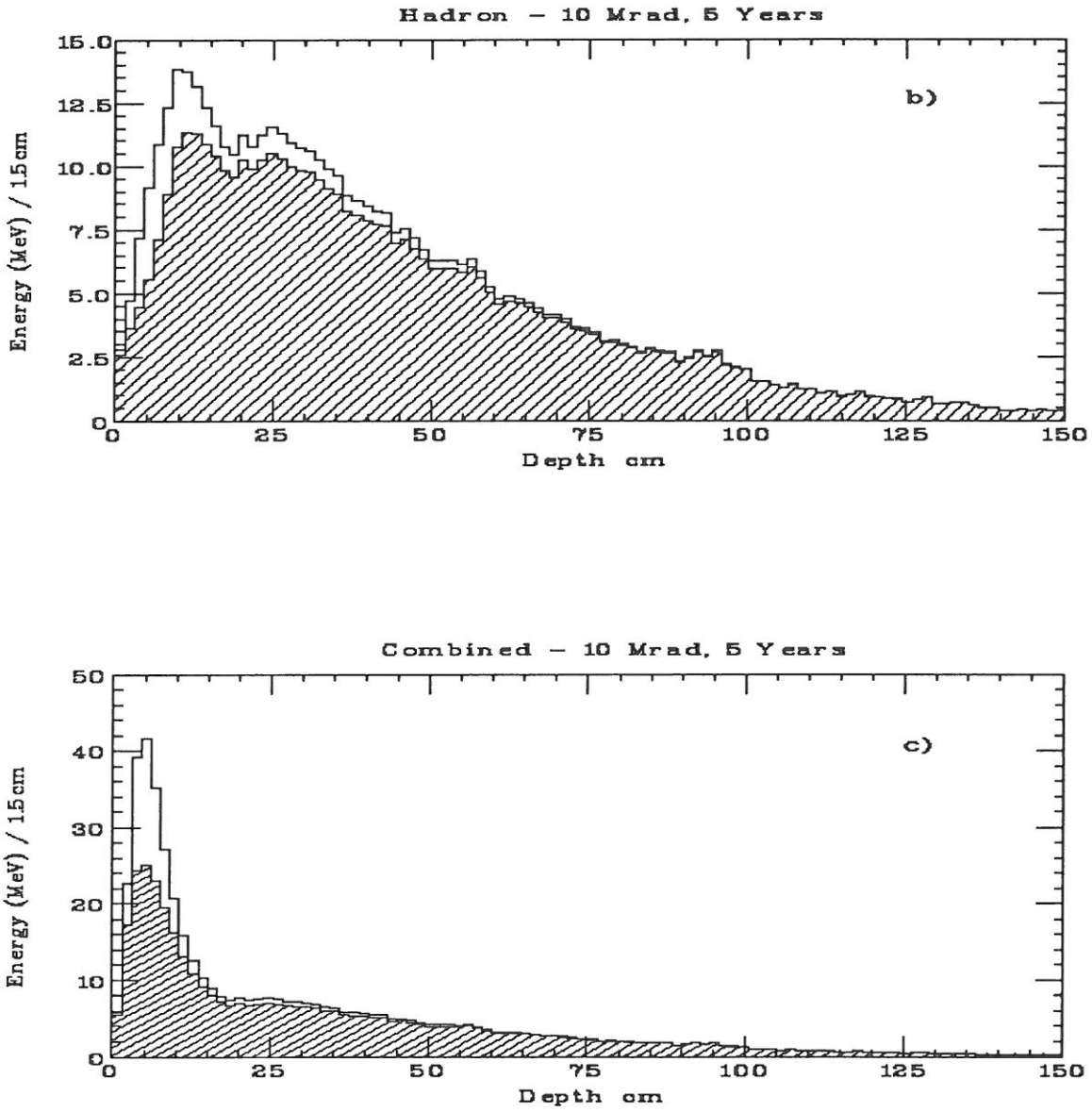

Fig. 2b) The unshaded histogram is the original hadronic signal, while the shaded represents the resultant signal after 5 years at 10 Megarads/year at 1% signal loss/Megarad/year. Fig 2c) Similar histograms for the combined signal. The shaded histograms in b) and c) have been done geometrically.

In the analysis programs, an average energy depth profile was calculated for the pions and the electrons. As can be clearly seen in the unshaded histogram in Fig. 2a, the electrons deposit almost all of their energy in the first 25cm of the calorimeter, whereas the pions(Fig. 2b) more uniformly deposit their energy throughout the calorimeter. From these respective profiles, a combined profile was obtained by adding one-third of the electron signal at a given depth to two-thirds the given pion signal at the same depth. It is

assumed that two-thirds of the energy entering the calorimeter at the SSC will be hadronic, while one-third will be electronic. The combined profile is shown in Fig. 2c.

As has been reported by others[1], the radiation dosage is not uniform in pseudo-rapidity. To take this into account, the plastic scintillator has been degraded by three different dosage rates, 5 Megarads per year, 10 Megarads per year, and 15 Megarads

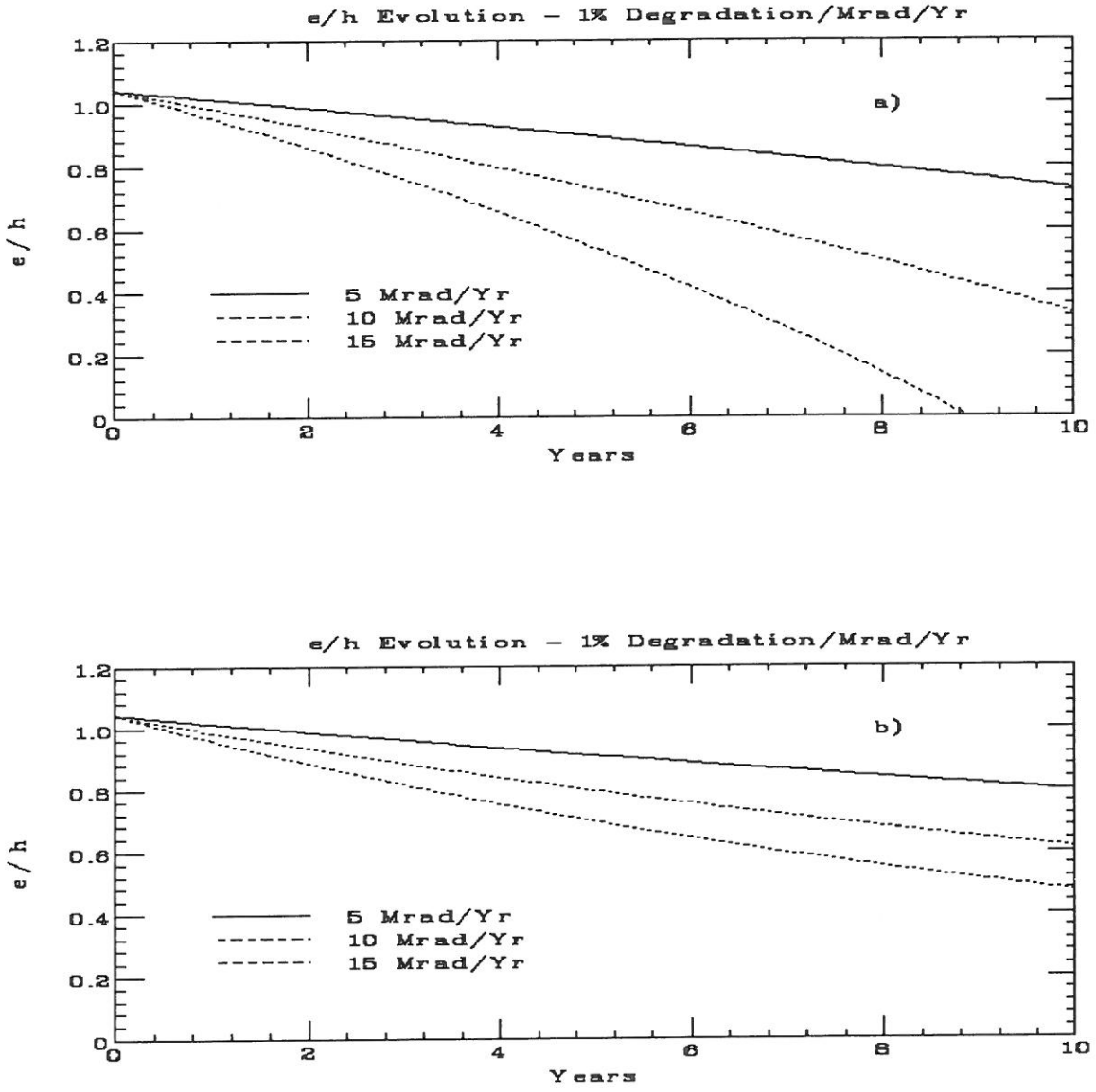

Fig 3. e/h evolution for a) linear degradation, and

b) geometric degradation.

per year. These dosages correspond to pseudo-rapidities that are values of 3 and larger. In addition, as has been reported at this conference, the degradation factor for plastic scintillator varies depending upon the type of scintillator used. Therefore, the plastic scintillator signal has been degraded by three different values, 0.2% net loss of signal per Megarad per year, 0.5% net loss, and 1.0% net loss. The time degradation of the scinitillator was carried out in two different ways. 1) A linear loss of signal: Effectively this means that the degradation builds up linearly with time, eventually reaching 100% for one particular case; and 2) A geometric loss of signal: This means the resultant signal is a percentage of the previous signal. The first method of course is the more severe case.

The peak of the combined distribution signal corresponds to the maximum dosage per year, and the other bins are accordingly scaled in dosage. The shaded histograms in Fig. 2 represent the resultant signals after an exposure of 10 Megarads per year for 5 years at a degradation factor of 1% done geometrically. As is readily seen, the electron signal is appreciably degraded, whereas the pion signal is hardly affected.This leads to a decrease in the value of e/h as a function of time.

In Fig 3a, the e/h evolution is presented as a function of time for a degradation factor of 1% done linearly for the three different dosage rates. As can be seen, e/h rapidly degrades for a dosage rate of 15 Megarads. After a period of two years, e/h has fallen from an initial value of 1.05 to values of 0.98, 0.92, and 0.86 for the dosage rates of 5, 10, and 15 Megarads, respectively. Therefore depending on the exact dose rate, the compensation characteristics have decreased by as much as 17% within two years. In Fig. 3b, the e/h evolution is given for geometric degradation. Here e/h has fallen to 0.99, 0.93, and 0.88 after two years, again for the same dose rates. Though not as bad as the linear assumption, the geometric case still shows a 15% decrease in compensation due to the plastic scintillator degradation.

3. Conclusions

As have been shown by the simulation studies, the compensation characteristics of a calorimeter that is part of a detector to be operated at the SSC will be severly degraded as a function of time due to the radiation doses encountered at the SSC. Our estimate that the plastic scintillator will recover to 99% of its signal output is currently over-optimistic. It therefore would seem that for a calorimeter to be useful, it will have to have design features that will enable the experimenters to quickly and easily **replace** the forward sections of the calorimeter, unless sufficiently radiation hardened plastic scintillator becomes available.

4. References

[1] D. E. Groom, Ed., SSC-SR-1033 (1988).

[2] T. A. Gabriel et al., "CALOR87: HETC87, MICAP, EGS4, and SPECT, A Code System for Analyzing Detectors for Use in High Energy Physics Experiments," Proceedings of the Workshop on Detector SImulation for the SSC, Argonne National Laboratory, August 1987.

T. A. Gabriel et al., "CALOR89: A Users' Manual," in preparation.

[3] R. G. Alsmiller Jr., F. S. Alsmiller, and O. W. Hermann, "The High Energy Transport

Code - HETC88 and Comparison With Experimental Data," Submitted to Nuclear Instruements and Methods..

[4] W. R. Nelson, et al., SLAC-265, Stanford Linear Accelerator Center, (1985).

[5] M. B. Emmett, ORNL-4972, Oak Ridge National Laboratory, (1975).

N. M. Greene et al., ORNL/TM-3706, Oak Ridge National Laboratory, 1973).

[6] J. O. Johnson and T. A. Gabriel, ORNL/TM-10196, Oak Ridge National Laboratory, (1987).

CAN A Pb/SCIFI CALORIMETER SURVIVE THE SSC?

D.W. Hertzog*, S.A. Hughes, P.E. Reimer, and R.L. Tayloe
University of Illinois at Urbana-Champaign, Urbana, IL 61801

K.F Johnson
Florida State University, Tallahassee, FL, 32306

and

S. Majewski, C. Zorn, M. Zorn
CEBAF, Newport News, VA, 23606

ABSTRACT

A scintillating fiber based electromagnetic calorimeter module built from radiation-hard materials has been tested in a beam capable of delivering both low and high currents of monoenergetic electrons. Energy resolution and light output measurements were made following high-dose exposures. The procedure was repeated until the resolution of the detector decreased from an initial value of $6.9\%/\sqrt{E}$ to $14.0\%/\sqrt{E}$ and the pulse height dropped by a factor of 11. After four weeks, the detector was retested. Partial recovery was observed in the light output which returned to approximately 52% of its original value. The resolution recovered to a value of $8.8\%/\sqrt{E}$. The tests are described.

1. Introduction

The use of plastic scintillating fibers embedded in a high-Z passive material such as lead is projected to result in a high-resolution, compensating calorimeter appropriate for a new generation of high-energy physics experiments [1]. The resolution is achieved by minimizing the sampling fluctuations. This is realized by the replacement of traditional scintillation plates with small-diameter fibers. Equalization of light output from the electromagnetic and hadronic portions of a hadronically-induced shower (compensation) occurs if the ratio of active to passive material is properly tuned. Several programs are underway [2] to develop such a device. In the interim, great success has already been attained with the development of similar, but smaller, electromagnetic calorimeters [3,4]. These have been found to produce the excellent resolution typically found in lead glass. For both hadronic and electromagnetic fiber-based calorimeters, radiation hardness is an attractive and possibly necessary feature for their widespread inclusion in detectors of the

---

* Invited talk presented at the Workshop on Radiation Hardness of Plastic Scintillator, FSU, March 19-21, 1990.

PACS Index: 07.20.Fw
29.04.Mc

future. This parameter is coupled directly, but not limited, to the survival of the root plastic scintillator.

Inherent to the success and utility of such detectors is the quality and performance of the scintillating fibers. Our direct experience is with a 300-element, fiber calorimeter array built using hundreds of kilometers of fibers [4]. The performance of this array greatly depends on the module-to-module uniformity and on the long-term stability of the light output and attenuation length of the fibers. These features are difficult to monitor in a large-scale module production process. Furthermore, they may degrade in a field of high-radiation in a manner which is not easily accounted for in the data analysis. The situation is more complex for the 2 m deep, dual-purpose electromagnetic / hadronic units proposed for the SSC or LHC environments [2]. The highest radiation doses will be localized to the electromagnetic compartment of the calorimeter. Since the fibers in such a calorimeter point toward the interaction region and extend, in part, from inside to outside, the ends nearest to the beam experience a much greater dose of radiation than the ends far away. If the light output of the scintillator slowly decreases due to radiation damage, the response of the front portion of the detector will differ from that of the rear portion for equal depositions of energy per unit volume. The calorimeter may be expected to demonstrate non-linear behavior and worsening of the energy resolution from such an effect.

Scintillating fibers produced to date have been made from a polystyrene core which is intrinsically more radiation resistant than other traditional materials such as acrylic. In part, this has prompted the label "radiation hard" as a characteristic of fiber calorimeters [3,5]. Additionally, both commercial and academic centers are intensely involved in the development of new plastics and fluors which are better suited for stability in the environment of high-radiation fields. Development of such plastics will extend the utility of plastic scintillator in all detector designs. For the moment, we must address the very important question, *"Can a present-day scintillating-fiber calorimeter survive the SSC?"*

The radiation field of the SSC, presented in the model of Groom [6], indicates a wide range in needed survivability versus pseudorapidity (η). With the assumption of ten years of operation at an optimistic luminosity of 10^{34} cm^{-2} sec^{-1}, the expected integrated dose in the electromagnetic compartment of a typical detector ranges from 0.25 megarad (Mr) in the central region at $\eta = 0$ to 50 Mr in the forward region at $\eta = 3.0$. This field is considerably higher than that of current generation, comparable experiments and stimulates new thinking for all detector components which are to be a part of any SSC detector.

We have tested the radiation hardness of a lead / scintillating fiber (Pb/SCIFI) calorimeter module made from state-of-the-art fibers and adhesives. This test was intended as a "proof-of-principle" that a highly radiation resistant instrument utilizing the techniques developed could be built. The spirit of the exercise is to alternately measure, irradiate and remeasure a detector using

the same source. The cycle is repeated until the performance of the detector has greatly deteriorated. The source is a 93 MeV monoenergetic electron beam at the University of Illinois Nuclear Physics Laboratory. The beam may be tuned to deliver alternately a narrow, low-intensity beam for resolution and light output measurements or a high-intensity, artificially diffused beam for the irradiations. Some evidence exists indicating nearly total recovery of the light output and attenuation length of some types of scintillating fibers when exposed to air after irradiations [7]. The calorimeter module we built was made from a particularly radiation-resistant fiber of this type. Since access to air was considered essential for rapid recovery, the module was constructed to permit air diffusion to the fibers. The test area was prepared carefully in order to make meaningful retests periodically after the initial runs.

Our program is largely complimentary to the dedicated fiber tests which have been reported at this workshop [8]. While a large variety of fibers can be tested using the "fiber only" methods, the motivation here is to compare results when a real detector is fabricated from a particular fiber and used in an environment which more closely simulates that of its eventual use. If this detector deteriorates at a radiation level below the dedicated "fiber-only" tests, then the question "Who or what do we blame?" must be addressed.

The tests described below show a rapid deterioration of the calorimeter performance with dose. Partial recovery of the pre-irradiation characteristics of the detector are observed after a period of four weeks from the initial irradiation runs. We are continuing to monitor this detector and are planning an additional test with a module made from a new type of "radiation-resistant" fiber.

2. Design Considerations

The Pb/SCIFI calorimeter blocks consist of a matrix of 1 mm diameter scintillating fibers embedded in a lead alloy, Fig. 1. The fiber chosen was a Kyowa, PTP/3-HF (green emitting) polystyrene fiber with an acrylic cladding which we had shown to recover in air to its original attenuation length after a dose of 10 Mr [6]. All fibers are aligned in parallel in the grooves of the plates shown in Fig. 1. They are surrounded by an adhesive which bonds the fibers and the plates in a "lasagne-like" structure. Since constructing a full hadronic calorimeter is impractical, we chose to make our tests with a smaller module optimized for its electromagnetic shower characteristics. This module is based on a well-understood design which has proven successful for us in the past [4].

The volume ratio of fiber-to-lead affects both the energy resolution and the equality of response to electromagnetic- or hadronic-induced showers (e/π ratio). These responses cannot be simultaneously optimized. While energy resolution improves with increasing fiber content, an e/π

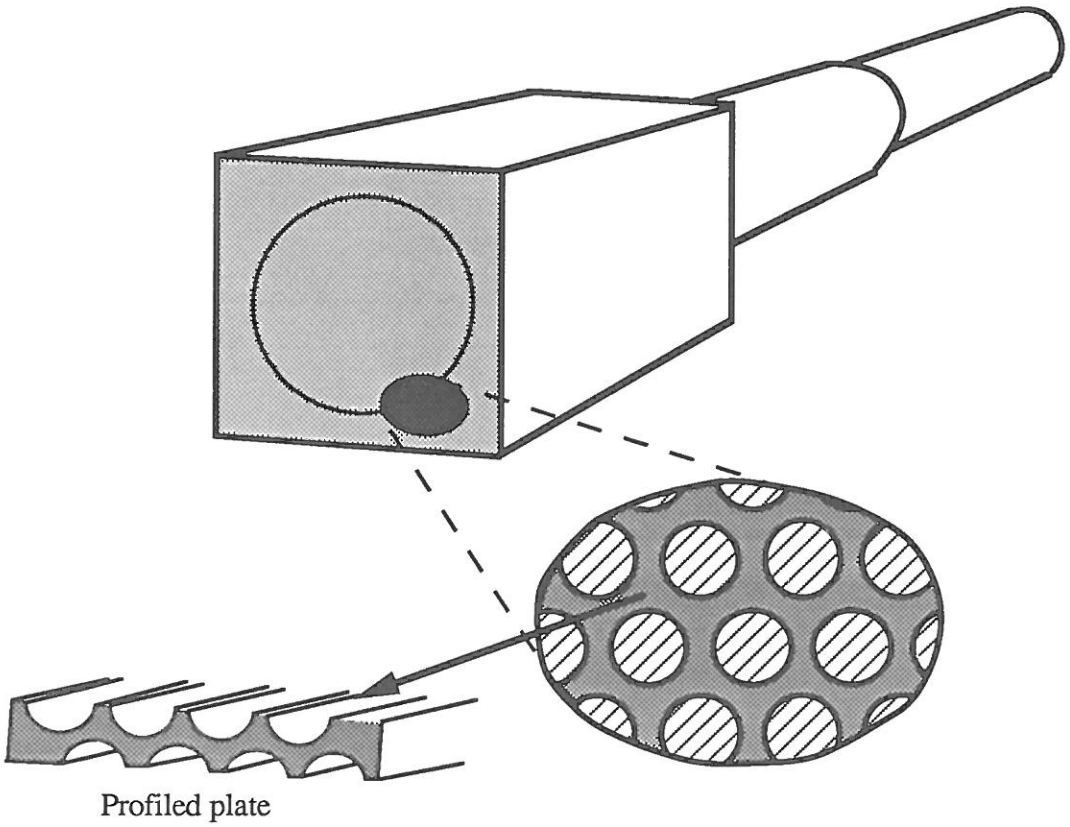

Figure 1
A Pb/SCIFI module is shown with the circle indicating the size of the lightguide which was attached to the downstream end. The enlargement shows the relative matrix of fibers, the construction of which is facilitated by use of a stack of profiled plates interwoven with scintillating fibers. See Ref. 4 for further details.

response of unity is expected when the ratio of fiber-to-lead is approximately 1:4 [1]. The ratio of fiber-to-lead in our (electromagnetic) design is 50 : 35, leaving 15% volume for filling around the fibers with an adhesive. The density of a finished block is found to be $\rho_{Pb/SCIFI} = 4.58$ gm / cm^3 leading to a radiation length of $X_0 = 1.61$ cm. The fibers are placed exactly on the corners of equilateral triangles with a fiber-to-fiber spacing of 1.35 mm, see Fig. 1. The test detector measured 9 x 9 x 22 cm^3 ($\approx 14\ X_0$) which is sufficiently long to contain the shower initiated by a 93 MeV electron.

The material used to fabricate the plates is an alloy of pure lead containing 6% antimony by weight. This has far superior mechanical properties compared to pure lead. Inside the grooves of each plate, the fiber is not in direct contact with air, but with the adhesive used to hold the plates together. To optimize the radiation-hardness of the detector, we found that standard optical epoxy

cements were unsuitable. Instead, we used Petrach Systems PS-273 encapsulant, a polymer of the polysiloxane family, which was chosen because

1) it remains clear up to 100 Mr,
2) its properties, such às adhesive ability and chemical inertness, are not significantly affected by radiation, and
3) it is highly permeable to air, allowing air to diffuse into the module to enhance recovery.

The detector was wrapped in aluminium foil to which several strips of copper tape were attached providing an electrical connection for current integration. If the block had been insulated, it would have accumulated electric charge and become charged to a high voltage. To avoid this, it was discharged to ground through a ballistic galvanometer. This allowed us to measure the total intercepted beam and, from that, to compute the deposited dose. The conversion to a dose scale is discussed below.

A 6.5 cm diameter by 10 cm long cylindrical Plexiglass lightguide was attached to the center of the rear face of the detector and a RCA 8850A photomultiplier tube viewed this lightguide. The light collection was designed to view only the central portion *within a* 6.5 cm diameter region of the module which we intended to damage. During resolution and light output tests, the current from this photomultiplier tube was digitized for each event. An event was defined by a pair of trigger scintillators; one of which had a 0.6 cm hole in the center and was used as a veto.

3. Test Runs and Results

The calorimeter was held in a mechanical cradle and was positioned 1 m downstream of the last vacuum pipe in the electron-scattering hall. The beam profile on the front face of the calorimeter was approximately 5 mm in diameter. This configuration was used for the resolution and light output runs, Fig. 2a. During irradiations, a lead foil diffuser was positioned at the downstream vacuum window of the last vacuum pipe to ensure that the beam was distributed uniformly over the face of the module. The diffused beam incident on the front face of the calorimeter was constrained to a 6.1 cm diameter circle by a lead collimator, Fig. 2b. The uniformity and alignment were checked by positioning a "placebo" calorimeter, an uninstrumented assembly of lead and acrylic scintillator sheets, where the module was to be irradiated. The placebo was irradiated and the scintillator sheets were darkened, providing a record of the beam uniformity and longitudinal shower profile. The beam was quite uniform across the 6.1 cm target circle.

a) Resolution and light output configuration

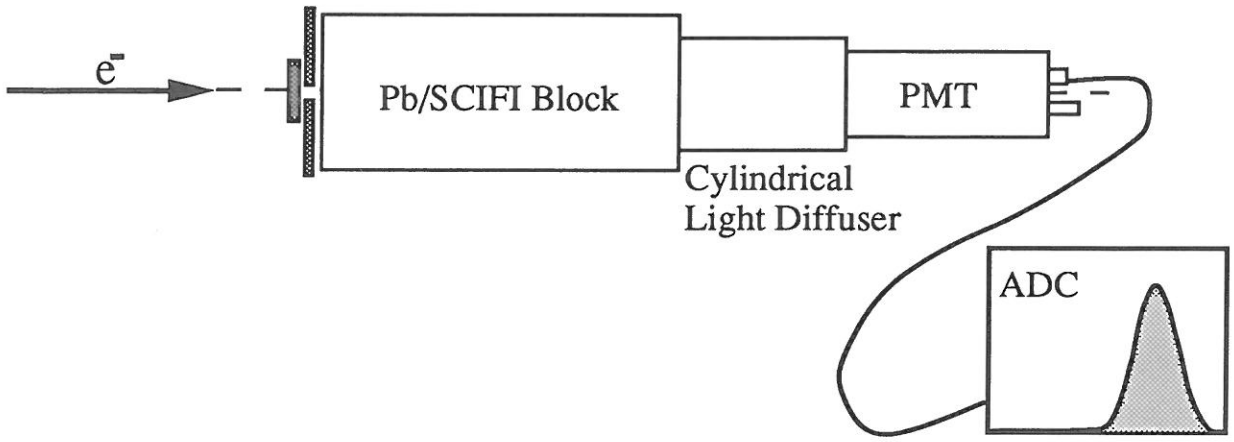

b) Irradiation configuration

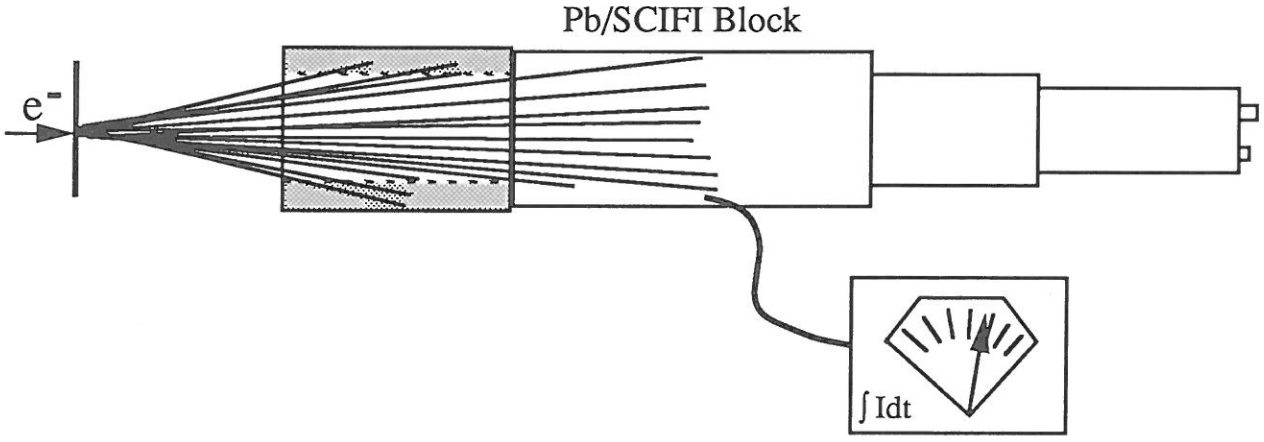

Figure 2

a) The basic setup used for the resolution and light output tests in which a well-focused monoenergetic electron beam is incident on the center of the front face of a Pb/SCIFI module. A histogram of the pulse height for each electron is formed using the trigger scintillators to gate an ADC. b) During irradiation runs, a beam diffuser is inserted upstream of the module and a collimator matched with the cylindrical lightguide is placed in front of the module to produce a uniform irradiation over the front face of the module. The current is integrated to calculate the accumulated dose.

The test calorimeter was then positioned and the electron beam was reduced in intensity to a rate of approximately (10-100) kHz. The resolution and light output were measured, where the absolute light output was determined by the use of a photomultiplier tube calibrated in photoelectrons (pe) per ADC channel. The typical light output for the undamaged detector was approximately 2700 pe / GeV. A pedestal-subtracted ADC spectrum for this run is shown in Fig. 3a. The mean of the peak is at channel 766 and the full width at half maximum (FWHM) corresponds to 405 channels. This represents a resolution of $6.9\%/\sqrt{E}$ with E in GeV when quoted in the format typical for sampling calorimeters. Our previous measurements with similar Pb/SCIFI detectors [4] demonstrate that a $1/\sqrt{E}$ scaling of the energy resolution is valid to very low energies.

Next, the trigger scintillators were removed, a lead collimator was inserted directly upstream of the module and an electro-mechanical table upon which the entire assembly was supported was remotely moved away from the beam line. The electron beam current was then slowly raised to a current of approximately 20 nA. Once stable, the table was repositioned in its original location and the irradiation was begun. The Pb/SCIFI detector was used as a Faraday cup to integrate the total charge. After approximately 15 minutes, the beam stop was inserted and the module was allowed to "cool" for an additional 15 minutes. The setup was then reconfigured for the resolution and light output measurements as described above.

This cycle of measurements was repeated until a total charge of nearly 400 μC was accumulated in the detector. The entire set of measurements was performed in a 36 hour period. In Fig. 3b, the pulse height spectrum from the last measurement is shown in which a greatly distorted peak is evident with a centroid at channel 71 and a FWHM of 77 channels. If the spectrum had a Gaussian form, this would correspond to a resolution of $14.0\%/\sqrt{E}$. The light output here dropped by a factor of 11 compared to that of the original undamaged detector. A plot of the resolution, expressed in "%"/$\sqrt{E}$ (left ordinate) and pulse height of the peak centroid (right ordinate) versus integrated dose in μC for all of the measurements is shown in Fig. 4. To determine the resolution parameter from the data, the FWHM was extracted by hand and was converted to an effective σ as if the detector maintained a Gaussian response. A true Gaussian response was only realized for the undamaged detector. The trend of both the resolution and light output is clear from the data in Fig. 4. Both parameters fall steadily up to an integrated dose of 200 μC. After that, the detector is so heavily damaged that the response changes more slowly. We attribute this to a near saturation of the damage in the portion of the detector where the shower is concentrated. After 200 μC, only the energy deposition in the tail of the shower is observed, presumably, in a portion of the detector with much less damage.

After four weeks, the detector was retested in the same configuration with no changes to the electronics system or beam configuration. The retested detector once again exhibited a near

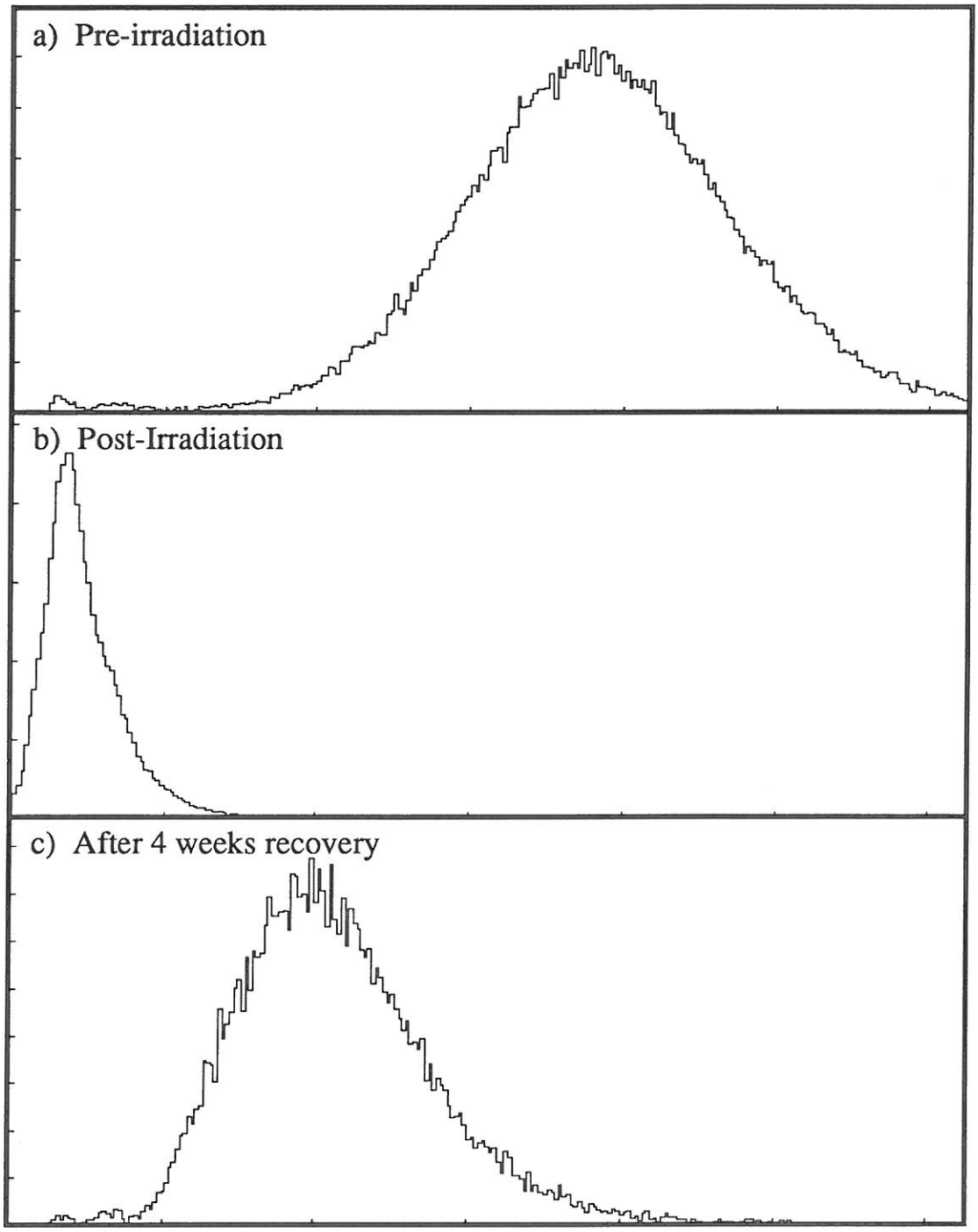

Figure 3
Detector response to 93 MeV incident electron beam before irradiation (a), after an accumulated charge of 400 μC (b), and after four weeks recovery time (c). The centroid of the peak represents the average light output which decreased by a factor of 11 during the irradiation period and recovered to 52% of its original value four weeks later. Similarly, the resolution deteriorated by a factor of 2 during the irradiation and recovered to 80% of its original value, see text.

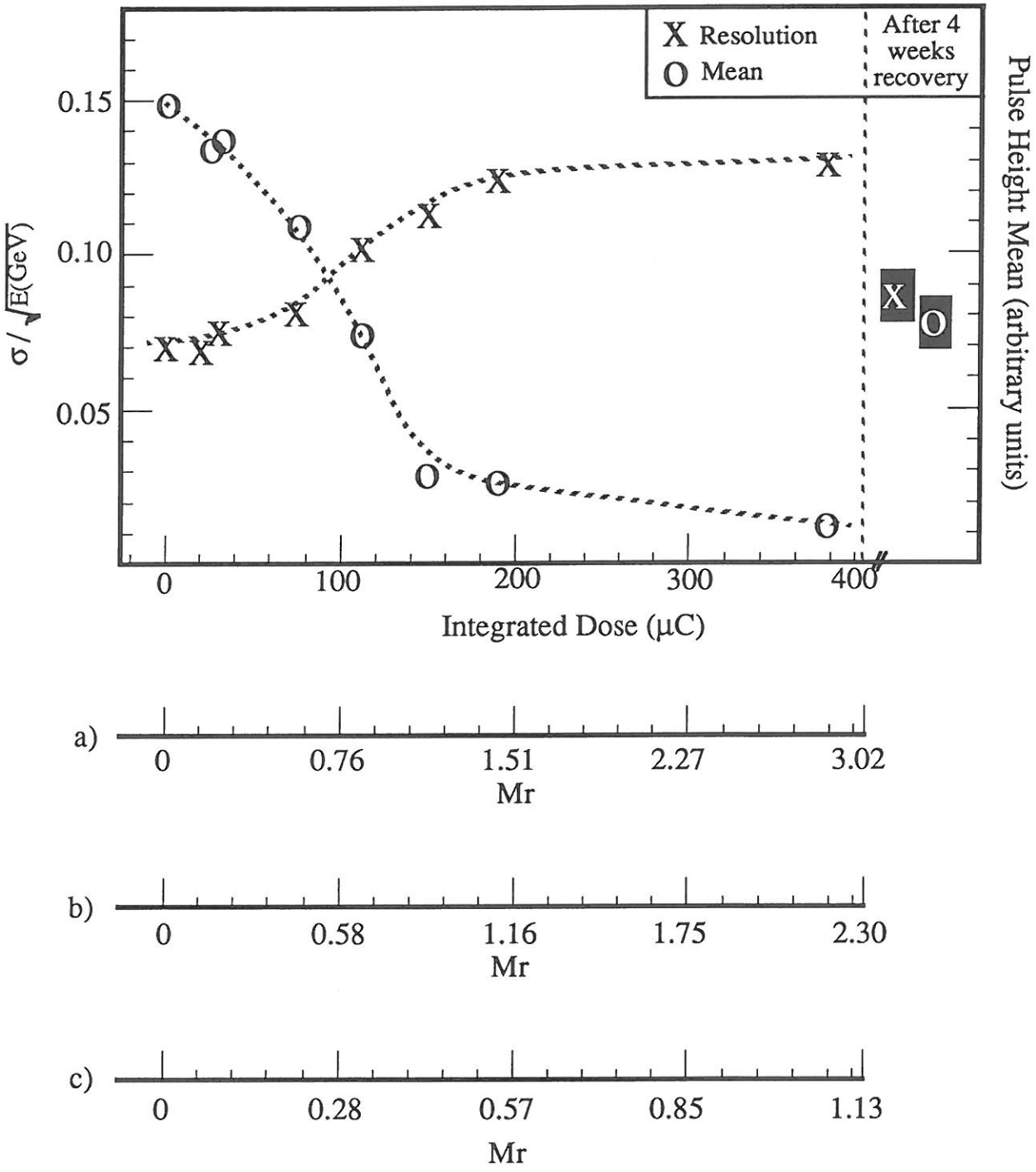

Figure 4

Resolution and pulse height mean versus integrated dose. The dashed lines are to guide the eye only. The separate scales represent calculations of the integrated dose in the regions a) ± 0.5 radiation lengths of shower maximum b) ± 1.0 radiation lengths of shower maximum and c) for the whole detector. The measurement at the right of the plot was made four weeks after the original irradiation and indicates partial recovery of the light output and substantial recovery of the resolution.

Gaussian response with a mean of 400 channels corresponding to 52% of the original light output, Fig. 4c. The resolution was measured as $8.8\%/\sqrt{E}$ which is nearly equal to that of the original undamaged detector. These points are indicated at the right in Fig. 4 and are labelled "After 4 weeks recovery".

The Rad is defined as an energy deposition per unit mass, namely; $1\ \text{Rad} = 6.24 \times 10^{10}\ \text{MeV / kg}$. Therefore, the abscissa scale conversion in Fig. 4 from μC to Mr involves a calculation of how much energy is deposited in a specific volume. The GEANT simulation program [9] with a full description of the detector geometry, including fiber, cladding, and adhesive, was used to determine the longitudinal energy deposition for an incident, monochromatic 93 MeV electron beam distributed uniformly over a 6.1 cm diameter circle on the front face and viewed by a 6.5 cm diameter lightguide on the downstream face. The integrated energy deposition in three regions about shower maximum was determined. The first region includes only the energy deposited in a band $\pm 0.5\ X_0$ around the shower maximum, resulting in a deposited energy of 18.5 MeV per incident 93 MeV electron. This occurs in a mass of 0.245 kg. We make the simple assumption that the energy deposition is uniform in a material of density $\rho = 4.58\ \text{gm / cm}^3$ and do not make additional corrections for relative deposition of energy in the lead or fiber. A 20 μC irradiation implies a deposition of 0.151 Mr in this band. The second band is $\pm 1.0\ X_0$ around shower maximum and leads to a deposition of 28.5 MeV per electron. The final region considered is the entire detector with a deposited energy of 86.2 MeV per electron. Since the longitudinal deposition is highly non-uniform, the latter calculation greatly underestimates the damage at the peak of the shower.

4. Conclusion

The three dose scales discussed above are displayed beneath the data in Fig. 4 and indicate that severe performance degradation had occurred after a short-term dose of 0.75 Mr. This would seem to be in contradiction to the tests on free fibers reported in reference [7], in which full recovery of attenuation length and approximately 90% recovery of light output were observed after 10 Mr. The recovery in the latter case was, however, for fibers in unrestricted contact with gaseous air for 10 days. In the present case, we have fibers in contact with a substance (the polysiloxane adhesive) in which the oxygen mobility, although two order of magnitude greater than standard epoxy-based optical cements, is still many orders of magnitude less than free air. A much retarded recovery in the present case can be expected. Still, the detector shows a dramatic recovery after four weeks annealing time. The level of light output, 52%, did not reach 90%, the recovery measured on free fibers, which we may take as an indication that the recovery process was not complete. We intend to retest the detector again in the near future.

The difference between our measurements and those performed on the individual fibers may lie only in the diffusion time of the air into the fibers. A direct comparison of the recovery time should be made between bare and embedded fibers in future "fiber-only" tests. As long as the annealing time can be kept short compared to the time over which the damage is accumulated, Pb/SCIFI calorimeters can be expected to remain fairly stable.

Returning to the question of survival at the SSC, it should be noted that any detector with stability up to 1 Mr will suffice for an η up to 2.0 ($\approx 30^{o}$) [6]. The tests reported here do not quite demonstrate that benchmark. However, they are not finished. Another post-irradiation measurement is planned. Our hope is to find a combination of materials that will result in a Pb/SCIFI calorimeter stable to 10 Mr.

Acknowledgements

We thank the staff of the University of Illinois Microtron for their expert operation of the accelerator and we thank M. Moushmof for his careful preparation of parts of the experimental apparatus. This work was supported in part by the U.S. National Science Foundation under contract NSF PHY 89 21146 and by the U.S. Department of Energy under contract DE-FG05-87ER40319.

References

[1] J.E. Brau and T.A. Gabriel, Nucl. Instrum. and Methods A238, 489 (1985) and R. Wigmans, Nucl. Instrum. and Methods A256, 273 (1988).

[2] The SSCINTCAL collaboration: Boston, CEBAF, Fairfield, Florida State, FNAL, KEK, Michigan State, Northeastern, Purdue, Rockefeller, Rutgers, Texas A&M, Univ. of California-San Diego, Univ. of Illinois at Urbana-Champaign, Univ. of Michigan, Univ. of Rochester, Univ. of Tsukuba, Univ. of Washington, Yale, and the SPACAL Collaboration: Cagliari, CERN, Lisbon, Max-Planck (Heidelberg), NIKHEF, Pavia, Rio de Janeiro, UC San Diego, and Weizmann.

[3] P. Sonderegger, Nucl. Instrum. and Methods A257, 523 (1987).

[4] D.W. Hertzog et al., *A High-Resolution Lead / Scintillating Fiber Electromagnetic Calorimeter,* ILL-(NPL)-90-001, and Nucl. Instrum. and Methods, in press.

[5] J. Kirkby, Proc. of the Workshop for the INFN Eloisatron Project: Vertex Detectors, Erice, Sicily, 225 (1986).

[6] D. Groom, these proceedings.

[7] S. Majewski et al., Nucl. Instrum. and Methods A281, 500 (1989).

[8] See the reports of A. Maio and K. Yasuoka, these proceedings.

[9] R. Brun et al., GEANT Reference manual, CERN DD/EE/84-1, Version 3.1305.

ELECTRON ACCELERATORS AS IRRADIATION FACILITIES

Stan Majewski

CEBAF, Physics Division
Newport News, VA 23606

ABSTRACT

Gamma irradiators have only a limited application in radiation damage studies of plastic scintillating fibers. Present experience and future plans point out to electron beams as convenient irradiation sources.

1. Introduction

At the present phase of planning for plastic scintillator-based detectors at the SSC, one of the crucial questions remains: will the radiation damage be the ultimate obstacle on the way of using this fast, efficient, easy to use and economical active material? This fundamental question of survival must be studied vigorously if the necessary proof of principle is to be delivered on time before the final decisions are to be made. The goal of the present contribution is to focus attention on the lack of satisfactory radiation testing facilities of scintillator samples and detector modules, and to make the point that the existing or planned electron beam sources may fill this gap already in the near future providing appropriate R@D planning by the SSC community is made.

2. Gamma irradiators and their disadvantages

The gamma irradiators remain with neutron irradiators the two main irradiation tools in studies of radiation effects in electronic elements and silicon detectors, as is discussed in many contributions to this meeting. Usually small transversal size beams delivered by these facilities are sufficient for the sample sizes involved and also because of the local character of the damage phenomena in silicon. There are many gamma irradiators located conveniently in the university centers, national laboratories, medical centers, naval research laboratories, etc around the country. The partial list of the gamma irradiators available to the outside users is listed in [1].

Past and present radiation damage studies of plastic scintillator materials also make use of these gamma irradiators.

However, they are limited to small-size samples in a preliminary evalution phase of radiation resistance studies, usually in the case of new plastic materials. A "classical" example of such an approach is the case of polysiloxane, a radiation-resistant polymer investigated for a plastic scintillator base. In all the studies conducted up to the present, only small-size samples were used [2].

It is well known [3], that the main effect of radiation on plastic scintillator materials is radiation-induced attenuation due to discoloration (color center formation) of the base plastic material. To study with sufficient precision the effect of this absorption on a final performance of the detector, the real-size samples of fibers, scintillating plates or waveshifting bars should be used. This in most cases precludes the use of gamma irradiators with their intrinsic limitation to active sample size. In some cases, the researchers attempt to remedy this limitation by use of several gamma sources in the same irradiation chamber or in other more complicated geometry arrangements. However, there still remains the limitation of rather inflexible range of irradiation dose-rates and doses which is not a free parameter but geometry (distance from the source(s)) related.

3. Experimental uses of electron beams in irradiations and the advantages of the technique

In contrast, the electron beams have all the flexibility required to irradiate long or large samples at different, regulated dose rates. The irradiation can be done uniformly over the sample size or following any other preprogrammed dose pattern. This additional and substantial advantage of electron sources will be discussed more in depth later.

The first preliminary irradiation studies of scintillating fiber samples for the SSC detectors were performed quite recently, utilizing the 3 MeV electron Van de Graaff accelerator of the Florida State University in Tallahassee [4]. In a relatively short time many different mostly 1 mm diameter fiber samples supplied by four major world producers were uniformly irradiated over 50 cm regions and their recoveries were studied in different gas atmospheres. From this comparison, several promising radiation-hard candidates emerged, while many other were found to be not acceptable for further study. An example of obtained results is shown in figure 1. Generally, this was the first convincing demonstration of dramatic differences in resistance limits of different available fiber types. Also, for the first time a clear separation of the attenuation losses and the intrinsic (local) radiation damage was possible by utilizing a method of screening a 1 inch wide fiber section from the electron beam (with a lead brick absorber) during irradiation.

Figure 2 shows the result of a scan of some fibers in this region. The step increase at the boundary of the screened section is caused by the difference in scintillation yield in the irradiated fiber and its non-irradiated section. The relative (percentage) value of this step is equal to the percentage loss of the intrinsic (as opposed to long range absorption loss) scintillation yield in the fiber material. Immediately after observing this phenomenon, a succesfull attempt to minimize this local damage effect was made in the green emitting fiber with the 3-hydroxyflavone (3HF) fluor (dye) by increasing concentration of the fluor (Figure 3). This and many other results of that study confirmed that electron beam irradiations are a very efficient and powerful tool in radiation resistance studies.

In a subsequent study with a 80 MeV electron beam of the University of Illinois Microtron [5,6], two small scintillating fiber/lead calorimetric modules were irradiated in an electron beam and the preliminary results have confirmed that the green emitting 3HF fiber selected in the first study is a much more radiation resistant than the traditional blue emitting fibers. Some results of that study are presented in figure 4 [5].

From the past experiences, only briefly described above, and the considerations about planned studies one can prepare a following preliminary list of advantages of electron irradiations:

- generally: possibility to irradiate long and straight samples such as fibers, fiber bunches, light-guide bars, and also large surface scintillator plates, etc.,

- ease and flexibility of control and monitoring of the beam profile and size, with scanning capability by means of standard beam optics elements; for example SSC-type damage profiles can be generated with high energy electron beams (to be discussed below),

- intensity regulation over many orders of magnitude (important in dose-rate studies),

- ease of dose monitoring (in the beam transmission mode) with a simple Faraday cup method.

3.1. Generation of the profile damage "a la SSC"

The most difficult case is the case of scintillation calorimetry at the SSC. Simulation of damage in laboratory conditions is close to impossible, as opposed to the fiber tracker situation, where predictions seem to be relatively straightforward. In our opinion an interesting possibility arises with the availability of higher energy electron beams of

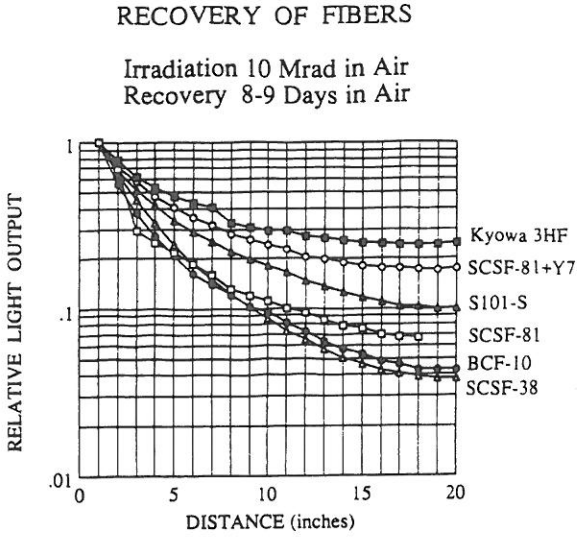

Figure 1. Comparison of fibers after irradiation to 10 MRad in air and after 8-9 days recovery in air. For each curve, the light output of the fiber at the position of 1.0 inches from its end has been normalized to 1.0.

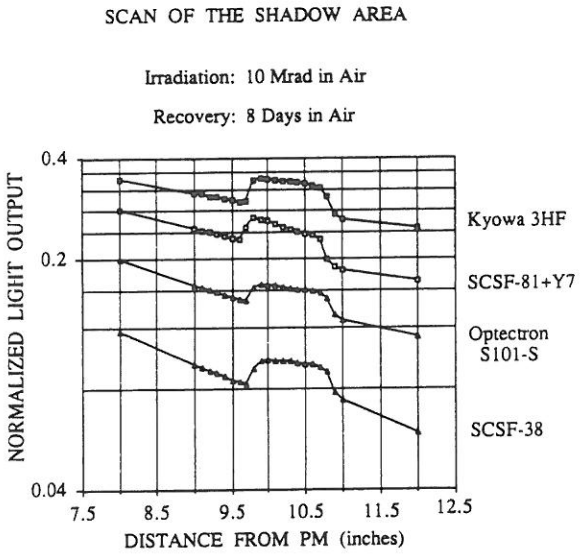

Figure 2. Effect of irradiation on local scintillation yield. Scan of screened region after 10 MRad irradiation in air and 8 days recovery in air of four fiber samples. A "jump" in the attenuation curve is produced by the damage to the local scintillation yield in fiber regions to the left and to the right of the screened unirradiated short fiber section.

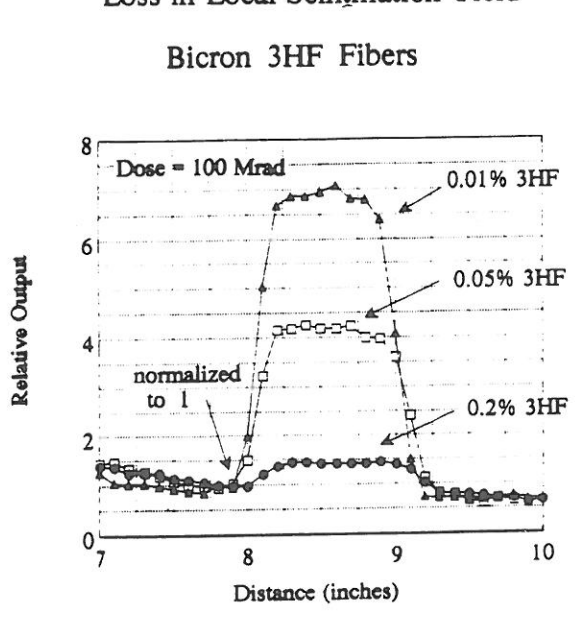

Figure 3. Comparison of damage to the local scintillation yield after a 100 MRad exposure in air and recovery in air for three different concentrations of 3HF.

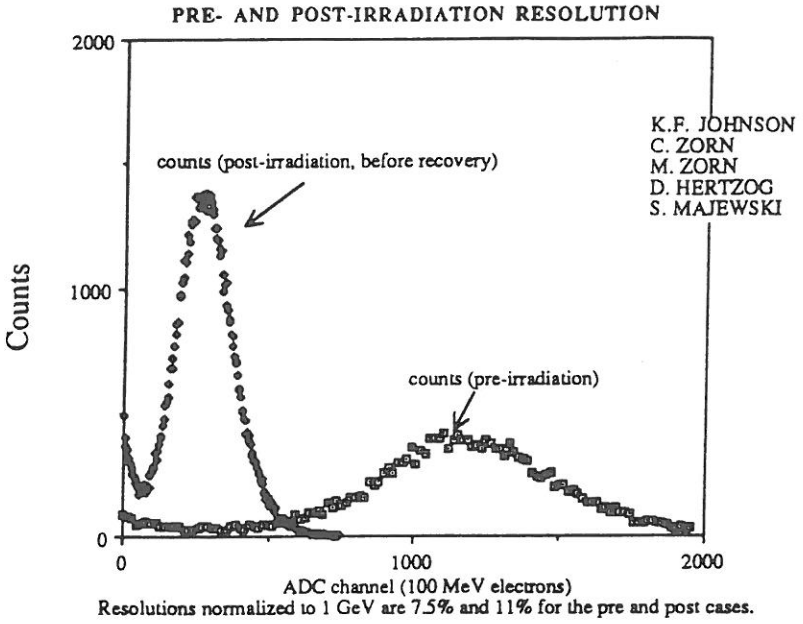

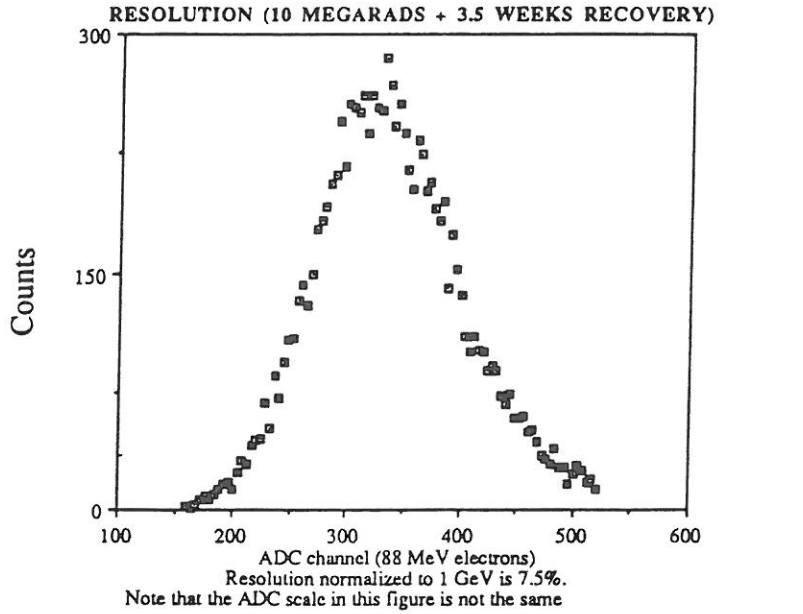

Figure 4. Pre- and post- irradiation resolution of a small calorimetric module made with 3HF fibers irradiated in a 100 MeV electron beam to approximately 10 MRad (upper figure) and after a 3.5 weeks recovery (lower figure). Note different energy scales.

the order of many hundred MeV and higher, and is presented here for consideration. From the simulations of the radiation field in the "generic" SSC detector [7], the expected radiation dose depth profile of a combined electromagnetic/hadron scintillating fiber calorimeter (or of a "son-of-Zeus" design, with scintillator/converter plate stack and with waveshifting bars collecting light) is well known. The dose distribution is very non-uniform with a strong and narrow maximum corresponding to a maximum in electromagnetic shower development and a broad, and deeply developed distribution due to the hadronic contribution.

A variation of this idea would be to first irradiate the fiber bunches before inserting them into a calorimetric module, and then testing the resulting performance of the "irradiated module" produced in this indirect way. This method avoids all the difficulty of securing the uniformity of transversal damage at a given depth of the irradiated module. However, it introduces an uncertainty in the time development of the extremely important recovery phase that takes place in fibers after the damage was made. This is caused by very different fiber handling conditions in this case as compared to the real-life situation, and especially their exposure to air.

This special technique of simulating damage in the SSC conditions, is expected to reproduce better the real situation if applied to the "son-of-Zeus" design. There, the properly pre-irradiated scintillator plates, would be inserted into the stack to form a full "irradiated" calorimetric module. Waveshifting bars, should also be irradiated with the correct depth-dependent dose pattern.

After preparing the fiber module or the plate module, the performance can be first tested with radioactive sources, LEDs, UV-light sources, cosmic rays, and/or the same electron beam used to induce the damage, but turned to a much lower intensity. For example, in the case of the 1 GeV electron beam the average position (depth) of shower maximum for electromagnetic showers is only a "logarithmic" distance away from the expected dose maximum. It will therefore probe the detector module response almost at the most damaged region of this calorimetric module. This beam test can provide crucial information enabling reliable evaluation of damage expected at the SSC, because the gained experimental knowledge can be in turn inserted into simulation programs to predict the effects of the damage on calorimeter detector performance.

Of course, to confirm the conclusions about expected radiation damage effects at the SSC from the damage effects produced and tested in the above proposed way, a "final" test in a high energy beam would be still necessary. However, by following the above procedure the proof of principle can be achieved much faster, as the requested (and difficult to obtain) high energy beam time would be limited to the absolute minimum to test only the final

number of preselected solutions, which passed the series of thorough electron beam tests.

3.2. Radiation dosimetry

To secure success of the proposed method a reliable radiation dose dosimetry to calibrate the dose distribution delivered to the plastic material is a must. Fortunately, such a technique exists. It is based on the use of a substance called alanine, the radiation effect on which is evaluated by the Electron Spin Resonace (ESR) method. This, by now well understood and precise dose calibration method, can be applied in the dose range of up to 10 MRad, being therefore an almost perfect match for the dose range used in the scintillator studies [8].

A set of alanine samples distributed along the irradiated sample, or inserted at several test points into the calorimetric module would provide an experimental dose and dose profile measurement, allowing for a test of the pre-irradiation calculations. Even more, this method can provide control of the total dose and dose profile well before the total planned dose would be delivered, therefore giving an on-line check of the correctness of the irradiation procedure. This can be achieved by dividing the whole irradiation into two (or more) irradiation periods, with the first, low-dose irradiation period serving as a control irradiation, after which the delivered dose-rate and dose profile would be cross-checked against the calculated (and desired) values. Therefore, if discrepancies are found, the necessary corrections to the irradiation procedure (and to the calculation package) can be made, so that the final result of the total irradiation is as close as possible to the planned one.

4.Available and planned electron beam facilities

In Table I the partial list of electron irradiation facilities is given in the order of increasing maximum beam energy (see also [1]). In general, these beams are adapted to deliver radiation doses much higher than the ones needed for the scintillator studies, but in most if not all the cases the dose rate (beam intensity per unit surface) can be lowered to acceptable levels. It is assumed that in the accelerated, time-compressed irradiation studies the highest acceptable equivalent dose rate in a scintillator sample is of the order of 1 Mrad per 5 minutes (up to 5 times higher dose rates were used in some tests), to avoid noticeable heating of material due to energy dissipation in the plastic. This translates into current densities of the order of nanoamps per cm*2 in the case of irradiation of fibers or fiber bunches (for traversing electrons, only a small fraction of their energy is absorbed in the sample material). Total beam current turn down can be accompanied by beam defocussing techniques, including beam scanning, to achieve this goal.

Table I. Partial list of electron beam facilities available for irradiation studies.

Energy	Facility	Location	Comments
2 Mev	Van de Graaff	Brookhaven	
3 MeV	- - - - - - - -	Lehigh U.	
3 MeV	- - - - - - - -	Florida State U.	
22 MeV	linac	Argonne N.L.	
45 MeV	- - -	Duke U.	available from 1990 (see text)
65 MeV	- - -	Naval Res. Lab., DC	
100 MeV	Microtron	U. of Illinois	no beam after 9/1990
100 MeV	linac	Nav. Postgrad. School, Monterey, CA	
1 GeV	linac	Bates/MIT	see text
1 GeV	linac	Duke U.	available end 1991 (see text)
4 GeV	2 linac sys.	CEBAF	available beg. 1994

4.1. High energy electron beams

Three high energy electron accelerators are especially promising as possible user friendly irradiation facilities.

The first one is the Bates 1 GeV linac accelerator. Very recently a test facility was proposed there to be used for the SSC detector R@D by several groups from the Boston area [9]. With only a modest upgrade of this facility radiation damage studies can be performed with electron energies up to almost 1 GeV. The only limitation is that the beams will be mostly available in a parasiting mode.

The second facility is being proposed by the Duke University group at the Free Electron Laser laboratory at Duke [10]. The proposed facility would be dedicated to detector testing and irradiation studies utilizing the 45 MeV and 1 GeV linacs of the FEL laboratory. The plan is to make beams available on an almost constant percentage beam time basis (about 20 %), and with all

the necessary logistical support available for any outside group wishing to use the facility. The proposed beam time structure of the 1 GeV linac can be made to simulate the SSC beam crossing interaction rate of 16 nanoseconds, so the time studies can be made at the same time when testing detector modules for other performance parameters, such as efficiency, energy resolution or radiation resistance limits. The expected date of completion of the test facility at Duke is by the end of 1991, providing the additional requested funding for the 1GeV test beam will be provided by the DOE and SSC.

Finally, the 4 GeV continuous electron beam accelerator constructed at CEBAF, Newport News, VA will be ready at the beginning of 1994, and it is being discussed what role it can play in the detector R@D for the SSC. It can be assumed that it will be possible to use its beam in some radiation studies, however the details will have to be worked out at a later date.

5. Some comments on test procedures

Several brief comments will be made here on the experimental procedure of radiation damage studies, which is of course interrelated to the problem of selection of appropriate irradiation facilities necessary for a complete and efficient radiation resistance study.

First, one must admit that the present situation is very confusing. There are many experimental results which to a large extent are not consistent with one another. The crucial question of the gas atmosphere effect on the radiation damage and recovery is still to be answered. There is no place here to review these results and discuss in depth the experimental evidence and possible reasons for discrepancies. Such reviews were recently done on other occasions, for example by Zorn [3]. It is exactly this unsatisfactory present situation that makes the present call for a very vigorous radiation damage R@D programme highly justified, if a proof of principle is to be delivered on time.

However, a list of following general suggestions can be made:

(i) continue tests with small samples (typically 1 cm cube) with gamma beams in a variety of gas conditions (air, argon, nitrogen, oxygen, etc.) and dose-rates (from the extreme of 1 MRad per minute to 1 MRad per 6 months or an even longer period); scintillator samples as well as pure plastic samples and waveshifter samples should be tested (for transmissional damage and recovery); this part of the study is particularly relevant to the plate stack calorimeter design ("son-of-Zeus"),

(ii) increase testing of life-size samples of individual detector elements such as fibers and fiber bunches or scintillator plates, light guides, light couplers,

waveshifting bars, and including effects of glues, cladding, etc.; this is when electron beams of several MeV are mostly useful; it can be claimed that some of the most important measurements cannot be made without these flexible irradiation tools, but still a comparison with gamma and fast neutron induced damage should be made for completeness,

(iii) finally, calorimetric modules including mechanical structure, with active material, cladding, glues, epoxies, light guides and waveshifters, light couplers, etc., and also with gas diffusion channels (as a possible solution to accelerate recovery) should be irradiated and tested in the high energy (many tens of MeV and higher) electron beams (or other high energy beams, if available) as was discussed above in subsection 3.1.; if possible, the irradiations should be performed at different dose rates to be able to extrapolate in a reliable manner the recovery data to the low dose rate SSC conditions,

(iv) to achieve this ultimate goal, the experimental studies should be accompanied by a thorough simulation effort to incorporate all the partial results of measurements and to be able to predict detector behaviour in the SSC conditions; also, at the same time the failure criteria for the detector performance should be defined from the simulation calculations, such as maximum acceptable light loss, attenuation increase, etc. consistent with not compromising detector parameters, such as efficiency, resolution, e/h ratio, etc.; preliminary efforts of this type were already initiated by several groups [11, 12, 13].

6. Summary

In summary, the combination of testing small scintillator samples irradiated with gamma sources with irradiations of individual fibers, fiber bunches, or scintillator plates and waveshifting bars, and finally of sections of full calorimeter modules in electron beams of up to 1 GeV and higher in energy, is expected to deliver in a relatively short time scale the necessary proof of principle for the plastic scintillator technique applicable to the SSC environment. An important part of the whole procedure is a reliable computer simulation package.

Electron beams in a many MeV energy range are already available and some new beams with interesting parameters and energy in a 1 GeV range may be made available to perform the outlined radiation studies. In view of importance of radiation damage studies for the proposed plastic scintillator detector R@D program, funding of some "user friendly" electron irradiation and test facilities seems to be a necessity in the present situation of a general lack of adequate irradiation and test beams for the SSC detector

studies.

References

[1] E. L. Petersen and P. W. Marshall, Standards for electronics radiation testing and remarks about SSC displacement damage testing, contribution to the meeting of the Task Force on Radiation Damage Testing at the SSC, Dallas, March 5-6, 1990,

also: J. C. Humphreys and C. M. Dozier, Cobalt-60 facilities available for hardness assurance testing, National Bureau of Standards report NBSIR 86-3480, November 1986.

[2] J. K. Walker, Polysiloxane scintillator, contribution to this workshop.

[3] C. Zorn, Studies in the radiation resistance of plastic scintillators. Review and prospects, invited paper presented at the 1989 IEEE Nuclear Science Symposium, San Francisco, January 21-26, 1990,

also: C. Zorn, Designing a radiation-hard plastic scintillator for high luminosity hadron colliders, contribution to this workshop.

[4] S. Majewski et al., Radiation damage studies in plastic scintillators with a 2.5 MeV electron beam, Nucl. Instr. and Meth. A281,500(1989).

[5] K.F. Johnson et al., High dose calorimetry with scintillating fibers, contribution to the 1989 IEEE Nuclear Science Symposium, San Francisco, January 21-26, 1990.

[6] D. W. Hertzog et al., Scintillating fiber calorimetry: performance/survivability, contribution to this workshop.

[7] D. Groom, Simulation of the SSC radiation field, contribution to this workshop, and references quoted therein.

[8] H. Schoenbacher, High-dose dosimetry and standarization of radiation tests, contribution to the meeting of the Task Force on Radiation Damage Testing at the SSC, Dallas, March 5-6, 1990,

also: F. Coninckx et al., Alanine dosimetry as reference dosimetric system in accelerator radiation environment, presented at the Second International Symposium on ESR Dosimetry and Applications, Munich, October 10-13, 1988, also CERN preprint TIS-CFM/216/CF, February 1989.

[9] E. Booth, A detector test area at the Bates linac, proposal to the SSC laboratory, and also private communication from Ed Booth, 1990.

[10] Al Goshaw et al., A detector test laboratory using a one GeV electron beam at the Duke Free Electron Laser Laboratory, proposal to the SSC laboratory, also private communication from Al Goshaw, 1990.

[11] D. Acosta et al., The effects of radiation damage on a scintillating fiber calorimeter, UC San Diego, Physics department preprint, 1990.

[12] J. Badier, Dose profiles/effects on calorimetry, contribution to this workshop.

[13] T. Gabriel and T. Handler, Damage simulations, contribution to this workshop.

RADIATION TOLERANCE IMPLICATIONS FOR THE MECHANICAL DESIGN OF A SCINTILLATOR CALORIMETER FOR THE SSC‡

J. Proudfoot
High Energy Physics Division
Argonne National Laboratory, Argonne, IL 60439

This paper discusses the issue of radiation damage in a sampling scintillator calorimeter with regard to the mechanical and optical design of such a device. Radiation damage is inevitable in some regions of the detector and the different damage and recovery time constants are compared to anticipated calibration data from W & Z Boson decays. Some plausible values for safety factors in the initial design are given.

1. Introduction

The radiation level in SSC interaction regions has been computed to be very large in some regions of the detector and poses a severe problem to calorimeter designers [1]. At the SSC design luminosity of 10^{33} cm^{-2} s^{-1}, beam-beam interactions result in a radiation level of 10 Mrad/year in a uranium/scintillator at a pseudorapidity of 3.0 and a radius of 2m. Moreover, physics may dictate the need to employ the highest luminosity attainable by the accelerator and the detector may therefore have to remain useable after several years of operation at luminosities approaching 10^{34} cm^{-2} s^{-1}. Even in the most optimistic scenario it is unlikely that any plastic scintillator will survive such doses unaffected. Therefore the challenge to a calorimeter designer intending to use this material as the detector medium is to incorporate the inevitability of degradation and the capability to accomodate it into the initial design.

2. The "Son-of-ZEUS" Calorimeter

Sub-system R&D [2] is currently being pursued to develop a design of a scintillator plate calorimeter with wave-shifter readout as an SSC detector. The objective is to develop a compensating calorimeter and therefore, as in the ZEUS calorimeter [3], a unit cell using Depleted Uranium (DU) is being evaluated. As a result, though many of the basic ideas are embodied in others of the current generation of large collider calorimeters (HRS, UA1, UA2, CDF), this design is now commonly referred to as the "Son-of-ZEUS" detector. The design team is following the well trodden path of:

Performance Specification
Design Life
Mechanical/Optical Design Implications
Detector Integration Design Implications
Mechanical/Optical Realisation

‡ Work supported by the U.S. Department of Energy, Division of High Energy Physics, Contract W-31-109-ENG-38.

The performance and design life are externally determined parameters (that is to say by the intending collaboration). The initial objective of this R&D effort is to produce a system based on conventional technology which can best meet them.

3. Radiation Damage Design Issues

A schematic of the optical configuration being considered is shown in Figure 1. This is shown in a perfectly projective layout and with a single waveshifter plate readout per depth in a tower. It is however to be understood that either the electromagnetic section alone or the whole calorimeter section must be tilted away from a fully projective angle to the interaction point to avoid light channeling effects in the waveshifter plates. Specific performance issues which must be addressed within the context of detector degradation under irradiation include:

- Initial light output
- Single sided rather than two-sided optical readout
- Number of depth readouts
- Cell size
- Resolution
- Uniformity both as a function of depth in the stack and point of impact
- Uniformity in Time
- System redundancy
- Calibration

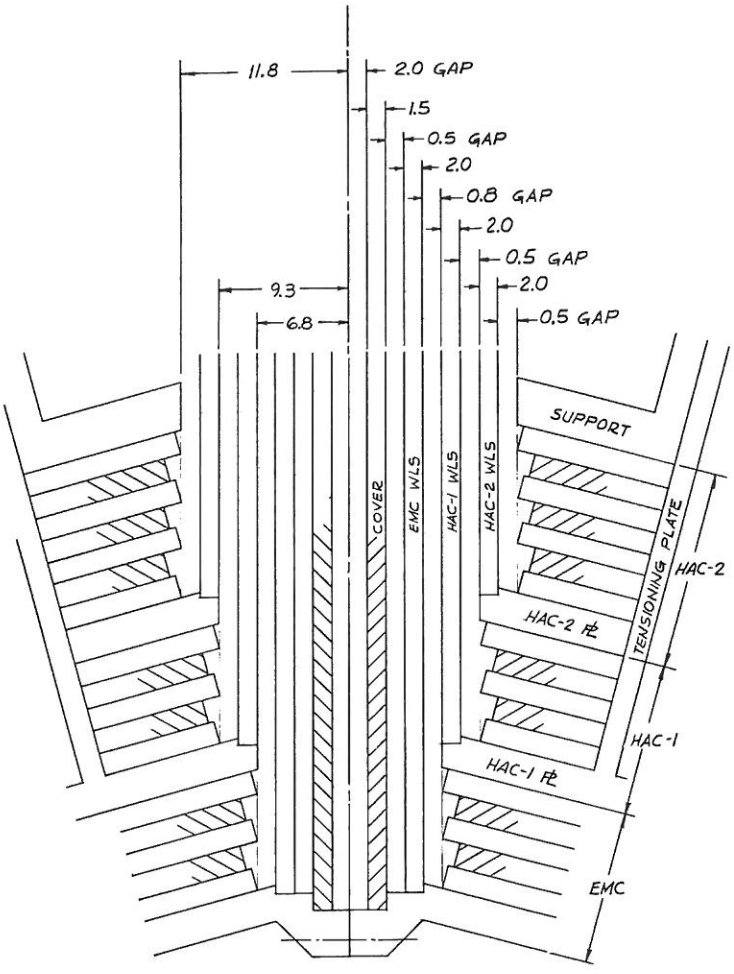

Figure 1

Illustration of the gap between module boundaries caused by wave shifter support structure and tolerances (dimensions are in mm). The effect of three readouts in depth is indicated.

First of all the higher the initial light output the more damage is required to attenuate the light yield to the point at which photo-statistics dominates the calorimeter resolution. Two-sided readout would allow both a level of redundancy as well as the capability of summing the two readouts to give a signal which is less affected by light attenuation in the scintillator (and hence a more uniform response in a system degrading under irradiation). Similarly multiple depth readouts in the damaged region, coupled with higher initial light yield would allow independent tuning of the relative gains to achieve uniform response in depth and position. Decreased cell size allows light to propogate a shorter distance in the scintillator and hence a correspondingly lower attenuation. However, all such options must be considered within the context of detector optimisation and are therefore not all realistic: two-sided readout coupled with small cells can greatly decrease the region of good electron detection efficiency; multiple depth readouts increases the number of electronics channels to be digitised and may greatly increase the cost of the device; increased light yield may in some cases only be obtained by reducing the level of compensation in the detector and hence the resolution of hadron showers. This is part of the design optimisation being carried out.

Calibration, however, is the key to continuing usefulness of such a detector operating in a dynamic cycle of damage and recovery. Although any such detector will be equipped with calibration systems to inject light and charge into the detector elements, the fundamental energy calibration will be provided by electrons from the decay of W and Z bosons in a fashion analogous to that used by the CDF collaboration [4]. These particles will be copiously produced having $\sigma \cdot B\ (W \rightarrow e\nu)$ of 8 nb and $\sigma \cdot B\ (Z \rightarrow e^+e^-)$ of 2 nb in pp collisions at $\sqrt{s}$ = 40 TeV [5]. The problem indeed for the experiment is to reject them.

It is straightforward to estimate the useful rate of such calibration events. Several factors may potentially reduce the raw rate and can be roughly estimated: trigger (x 0.5); transverse energy cuts (x 0.7); fiducial cuts (x 0.7). However, even in this relatively pessimistic scenario, the IVB calibration signal would be almost 3Hz at the SSC design luminosity of 10^{33} $cm^{-2}s^{-1}$. The calorimeter being considered has a stochastic term in the resolution function of approximately $20\%/\sqrt{E}$. Therefore, 100 events in a cell would provide a response calibration with a statistical error of only 0.4% (for a nominal electron transverse momentum of 40 GeV from W decay). This is comfortably below the desired non-uniformity of 1%. The lepton decay distribution is sufficiently uniform in the rapidity region $|\eta| < 3$ that therefore the entire calorimeter could be calibrated to this accuracy in only 15 days. The only minor difficulty is that this book-keeping and analysis would most likely have to be done on the fly in the level 3 trigger processor system as the rate is too high for data to be written to an output medium for post-processing.

This approach to calibration introduces another time constant into the system as the calorimeter response must remain uniform to within the precision of a single measurement (4%) for the 15 days required to accumulate IVB calibration data. This must remain true in an experimental situation with periods of collisions during which irradiation is taking place interspersed with down periods (for filling, M&D etc.) during which recovery potentially takes place. Therefore, the maximum variation in response must also be < 4% for a single store (for example, a situation in which the loss of light was 15% during a single store followed by 14% recovery during an M&D period would not allow the above precision to be attained). Ideally, one would wish for a system with a

long damage time constant and short recovery time constant such that dynamic equilibrium between the two processes would be attained during a store.

4. Conclusions

Radiation damage to a scintillator calorimeter at the SSC is eventually inevitable in important rapidity regions of the detector. Results presented at this workshop demonstrate that already there is reasonable understanding of the damage and recovery mechanisms and in the future there should be sufficient understanding to allow a reliable prediction of their time dependence in the actual detector environment. However, even plastics available today do not turn brown instantly (and better ones are promised). Therefore, a viable design philososphy to deal with radiation damage is:

- Track It
- Correct for It
- Eventually Replace it Where Necessary

The initial optical system design must include appropriate safety factors to allow this approach. These include increasing the initial light output over that mandated by photo-statistics (a minimum increase of a factor of 4 is indicated); an initial design with a higher resolution than necessary for the resolution of the Z width (a factor of 3 increase seems achievable); and multiple depth readouts in the regions of the detector susceptible to radiation damage.

References

[1] D. E. Groom, Editor, Radiation Levels in the SSC Interaction Regions, SSC-SR-1033.

[2] E. Ros, Editor, The ZEUS Detector Status Report 1989 (unpublished).

[3] H. Spinka et al., Development of a Compensating Scintillator Plate Calorimeter System for the SSC, ANL-HEP-TR-89-111.

[4] F. Abe et al., Measurement of the Mass and Width of the Z Boson at the Fermilba Tevatron, Phys. Rev. Lett **63**, 720 (1989).

[5] E. Eichten, I. Hinchliffe, K. Lane, and C. Quigg, Rev. Mod. Phys. **56**, 579 (1984).

RADIATION DAMAGE OF THE CDF BEAM-BEAM COUNTERS DURING THE 1988-89 FERMILAB COLLIDER RUN

N. D. Giokaris
The Rockefeller University
New York, NY 10021

ABSTRACT

We have measured the attenuation length and the light yield of some of the CDF Beam-Beam scintillator counters after the end of the 1988-89 collider run at Fermilab. A significant reduction in both these quantities has been observed.

1. Introduction

Some of the CDF Beam-Beam scintillator counters, henceforth called BBC, as well as one not exposed scintillator of the same material, have been measured with a ^{90}Sr radioactive source and with cosmic rays. In section 2 we describe the CDF BBC system. In section 3 the measurements and the results are given. In section 4 we attempt to give an estimate of the radiation dose received by the BBC. In section 5 the conclusions are listed.

2. CDF BBC System

The Collider Detector Facility (CDF) experiment at Fermilab has used the BBC system to provide a fast antiproton-proton (pbar-p) collision vertex finder and a minimum bias trigger and to serve as luminosity monitor. The BBC system consists of two planes of scintillator counters, one forward and one backward at a distance of 6.5 feet from the pbar-p interaction point. Each plane consists of sixteen separate counters and each counter is being viewed by two photomultipliers, henceforth called photomultipliers A and B. A schematic view of one of the BBC planes is shown in fig. 1. Note that each plane has a four-fold azimuthal symmetry. In Table I the radial, zenithial and pseudorapidity coverage of each of the counters is listed as well as their width and length. In Table II the sizes and the types of the corresponding lucite light pipes are listed. The scintillator type of the BBC is SCSN-23 [1]. Their thickness is one inch. For a more detail description of the BBC see Refs. [2,3,4].

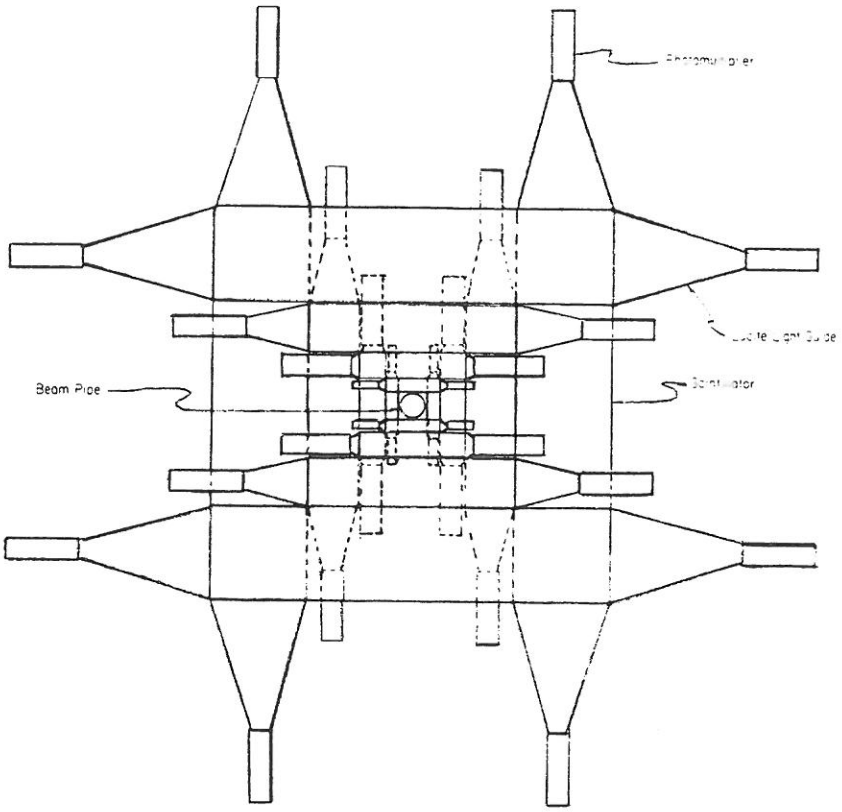

Fig. 1. Schematic view of one of the BBC planes.

Table I. BBC Geometrical Coverage and Dimensions

Counter #	rmin (in)	rmax (in)	θmin (deg)	θmax (deg)	ηmax	ηmin	width (in)	length (in)
0	1.31	2.54	0.32	0.62	5.90	5.23	1.23	5.09
1	2.54	4.93	0.62	1.19	5.23	4.56	2.39	9.87
2	4.93	9.56	1.19	2.31	4.56	3.90	4.63	19.24
3	9.56	18.5	2.19	4.48	3.90	3.24	8.94	37.00

Table II. BBC Lightpipe Dimensions

Counter #	Lightpipe Length (in)	Counter end Width (in)	Tube end Width (in)	Physical type
0	9/16	1.23	19/32	flat
1	3/4	2.39	1 3/4	flat
2	6	4.63	1 3/4	Double taper
3	12	8.94	1 3/4	Double taper

3. Measurements-Results

The measurements, mentioned in this paper, were perfomed after almost seven months after the end of the 1988-89 collider run at Fermilab. The BBC were removed from the collision hall after the end of that run. Although we did measure counters of all types i.e # 0, 1, 2 and 3 from both the forward and the backward planes [5] we will focus here on the comparison of a type # 1 BBC scintillator and of type # 1 scintillator from the same batch that was not exposed to radiation. These two scintillators were measured with the same photomultipliers at the same high voltage and with the same light guides. The current of photomultiplier A versus the ^{90}Sr source distance from light pipe A is shown in fig. 2 . The difference in current between the two scintillators at zero

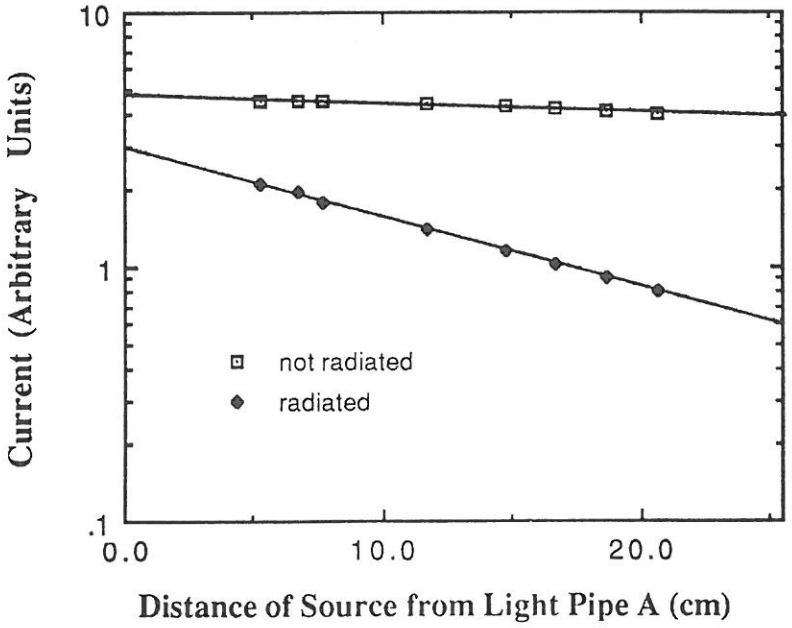

Fig. 2. Current of photomultiplier A versus the source distance from light pipe A.

distance should measure their difference in light yield. We find that the light yield of the radiated scintillator is about 40% less than the not exposed one. The attenuation length of the not radiated sample is (109+-15) cm to be compared with (15+-1) cm of the radiated one. Similar results were obtained by measuring the current of photomultiplier B. The measurements with cosmic ray minimum ionizing particles are in very good agreement with the ^{90}Sr source measurements. It should be noted here that because of the high multiplicity of the particles produced in a 1800 Gev pbar-p collision the deterioration of the BBC in the 1988-89 run did not have any adverse effects on its role as level zero trigger provider and luminosity monitor.

4. Radiation dose received by the BBC

The BBC system has been exposed to radiation during two collider runs. The first run lasted a short time period and the luminosity was rather small. By looking at the BBC pulseheight distributions, we can safely conclude that the BBC did not suffer any radiation damage in the first run. The second, 1988-89, run lasted longer (almost a year) and the integrated luminosity delivered by the accelerator was 10 pb^{-1} or about 200 times that deliverd in the 1987 run. This corresponds to a radiation dose, from pbar-p interactions, received by the type # 1 BBC scintillators of only 0.1 Krad. However there are other sources of radiation like beam-gas interactions and beam losses upstream and downstream the BBC. Indeed, PIN diodes and TLD' s installed, about two months after the BBC installation, closer to the interaction point than the BBC, indicate [6] that the lower limit of the radiation dose, received by the type # 1 BBC, could be 2 to 4 Krads. Significantly more radiation could have been seen by the BBC, before the installation of the PIN diodes and the TLD's, especially from total beam losses that did happen, close to the CDF detector, early in the 1988-89 run. However radiation dose of the order of 10 Krad, delivered at a relatively small rate, has been reported [7] to have caused significant damage to three types (BC-408, BC-412 and BC-434) of Bicron Corp. scintillators and to an SCSN-38 type scintillator. Also it was reported in this conference [8] that relatively small amount of radiation, delivered at a small rate over a long period of time, did have disastrous effects on plastics.

5. Conclusions

An SCSN-23 type scintillator of the BBC system from the CDF experiment at Fermilab has

been measured with a ^{90}Sr source and with cosmic rays after being exposed to 2 -> 4 Krad (lower limit) radiation. It was found that its attenuation length is 5 times shorter and its light yield 40% less than a control scintillator sample of exactly the same type and size. This damage could have been caused by a total beam loss close to the CDF detector. If this is not the case, we are forced to conclude that the damage was caused by a relatively small dose of radiation, delivered at a very small rate over a long period of time.

References

[1] KURARAY CO., LTD., Shuwa Higashi-Yaesu Building, 9-1, 2-Chome, Hatchobori, Chuo-Ku, Tokyo, 104 JAPAN.

[2] H. J. Frisch et al., CDF note # 250.

[3] T. M. Liss et al., CDF note # 552.

[4] F. Abe et al., Nucl. Instr. and Meth. A271 (1988) 387-403.

[5] N. Giokaris, CDF note # 1214.

[6] R. J. Yarema, Fermilab TM-1610.

[7] C. S. Lindsey et al., Nucl. Instr. and Meth. A254 (1987) 212-214.

[8] R. L. Clough et al., "Radiation Effect on Scintillating Fiber Optics for SSC", These Proceedings.

SUMMARY

Kurtis F. Johnson
Florida State University
Tallahassee, Florida

ABSTRACT

Even though clarifications are still needed in the data, and although the long-term behaviour of irradiated scintillator still has yet to be determined, there has been very substantial progress in the preceeding year. In particular, the following developments are important.

1) The "better red than dead" stratagem of utilizing long wavelength fluors whose emissions bypass the absorption by color centers has brought about an order-of-magnitude increase in radiation hardness of scintillator.

2) The quality of scintillator is approaching the level required for the electromagnetic section of the calorimeter barrel and has reached the level necessary for the hadronic section. This is true for the projected lifetime dose when it is received in a short time. Whether it will hold true for the same dose spread over a ten year lifetime has yet to be determined.

3) The single most important goal to reach in the near future, is to find a model which faithfully predicts, from high-rate irradiations, the long-term, low dose-rate behaviour of scintillator.

1. INTRODUCTION

Sketching a coherent picture at this juncture of the effect of radiation on plastic scintillator may be an impossible task, given the incomplete and, at times, contradictory nature of the evidence.

For example, it is remarkable that in spite of a considerable effort, there is still no clear understanding of the desirability of immersing scintillator in oxygen. It is certain that flushing with oxygen will induce rapid annealing of color centers, leading to a more transparent scintillator. It is not known, however, if annealing occurs in the absence of oxygen. It seems to, though at a more leisurely pace. However, this may be due to residual oxygen [Zorn, fig 1].

Some of the uncertainty is due to experimental difficulties. Air diffuses into plastic; isolating the effects of oxygen or other gases requires complete degassing of the scintillator. This can take many days and must be followed by irradiation and measurement in an anaerobic environment. This is certainly possible, but slow and expensive.

Thus, at the Workshop we have heard contradictory reports on the effect of nitrogen on recovery [Maio, Yasuoka - not received in time for publication].

It is also known that heating scintillator up to near its glass transition temperature greatly accelerates annealing, but it is not known why.

It is still an open question whether the annealed color center remnants in these two cases are identical. And there is the well founded, but unproven, suspicion that over several years, low dose-rate exposure in the presence of air is an order of magnitude more damaging to scintillator than the same dose delivered in a short time period, as is the case with mechanical and electrical properties of polymers. The presentation by N. Giokaris at the workshop of a

case of severe damage to scintillator which may be due to a low dose given over an extended time is very alarming.

2. FLUORS

A more optimistic development is the, meanwhile general, recognition of the utility of large Stokes' shift fluors, such as 3-HF (3-hydroxyflavone). The advantages for any large device, ie. one in which the optical signal must be transferred across meter distances, of a low self-absorption fluor and a wavelength in the green or longer, thus in large part bypassing radiation induced color centers, are too great to ignore.

I refer the reader to Zorn, fig. 1, which are typical examples of transmission spectra from damaged plastic. Transmission damage always is more severe at the blue end of the spectrum than at longer wavelengths. Clearly, the most robust scintillator is one which emits in the red, but the lack of a cheap, reliable and radiation insensitive photodetector make this option, at present, infeasible.

There is a second, more subtle, point in connection with large Stokes' shift fluors. Their low self-absorption property allows to increase the concentration of these fluors far beyond that of standard fluors without making a scintillator opaque to its own emitted light, and this can be used to stabilize the light yield at high doses [Zorn, fig. 7].

Although 3-HF, because of its oxygen sensitivity and low light yield, is unlikely to be the fluor of choice, it is very likely that these principles will be incorporated into new scintillator designs.

There is a very substantial ongoing effort, as evidenced by the presentations at the Workshop, to develop new fluors and to reassess the known fluors. Virtually every chemist active in the field seems to be building a new, large Stokes' shift, high quantum yield fluor [see Clough, Kasha, Kauffman, Harmon]. In addition, Clough is systematically testing dozens of fluors and bases for radiation survivability.

A variety of chemical families are being called into service for this purpose. This is a very positive development, for it means that in two years or so, when designs must be concrete, that we will have a more extensive palette of fluors with which to compound the scintillator we need. This wide variety of chemical species available for selection will increase the likelihood of finding suitable base/fluor combinations, since not every fluor will dissolve in a selected plastic base material in the concentrations needed to make a successful scintillator.

3. BASES

On the other hand, only three groups were represented which reported to be either attempting to find more resistant base materials or to researching the chemical bases of color center formation and annealing. Of these three, two were commercially oriented and not releasing information to the public.

This situation is suboptimal. There are two important reasons for investing resources into the clarification of the chemistry of color centers.

The first is a reduction in the number of variables. A listing of variables known to affect scintillator performance and radiation hardness includes: gas atmosphere or chemical environment during and after irradiation,total dose,

dose rate, temperature during irradiation, temperature after irradiation, physical dimensions of the scintillator, and, of course, scintillator type. There may be others. Mechanically stressed plastic, as from the differential expansion of scintillator-metal structures, or bent scintillator pieces, may be especially susceptible to radiation damage or radiation induced crazing. And very recently it was shown that thermal treatment of scintillator for even a few hours at moderately elevated temperatures (54° C) before irradiation will drastically reduce its radiation hardness [author's laboratory, July, 1990]. Thus, to the list above we must also add the pre-irradiation history of the scintillator.

Even the most diligent and tenacious experimentor cannot step through this multidimensional space of variables with any kind of useful resolution. There are simply too many variables. In-depth understanding is not to be had this way and the reliability of radiation damage measurements on a given scintillator will suffer from the uncertainty introduced by uncontrolled variables.

However, once the chemistry of color centers is understood and once the time and temperature dependence of annealing is understood, variations in measurements due to temperature, oxygen concentration or, possibly, relative humidity, can be accounted for by computation, allowing reliable comparisons of data between groups and definitive conclusions.

The second reason is that we have about two years until a calorimeter design which is to have a projected life of ten years is finalized, and at present we have no certain knowledge of how to conduct reliable accelerated damage tests, or of how to extrapolate the tests we have done to order-of-magnitude greater time scales. In other words, are the presently conducted damage tests, in which irradiations are conducted within minutes or days, relevant to behaviour which occurs on a decade time scale?

4. CALORIMETRY

There is progress in the "top down" design of calorimeters for radiation resiliance. That is, systematic investigation into optical and mechanical design with intent to minimizing the effects of radiation damage [Proudfoot]. We can expect comparative simulations of different detector geometries and the effect of radiation damage on, say, electron isolation, energy resolution, e/h, noise levels, etc. will become part of any engineering design study, in a continuation of the work begun by Gabriel, Handler and Badier.

At present, the damage function inputs (i.e. change in attenuation length and local light yield from radiation damage) used in the simulations are idealized. They do not utilize the time/temperature/gas environment/dose rate dependent damage and recovery, because this information is not yet available. Hopefully, by the time calorimeter designs begin to gel, it will be.

It is important that radiation damage considerations be integrated into the design process at an early stage, so that optimal fluor/base combinations which fulfill the performance specifications can be sought. Clearly, a scintillator plate and waveshifter bar type of calorimeter will be optimized for radiation resiliance with different fluors, concentrations and possibly base materials, than a scintillating fiber calorimeter.

There is room for optimism for scintillating calorimetry. Simulations reveal that the expected dose maximum to the scintillator in the electromagnetic calorimeter barrel is less than 1 Megarad at 10^{34} cm^{-2} s^{-1} luminosity after ten years [Groom]. Measurements on individual fibers indicate that for short term exposures a goal of less than 15% light loss at this exposure level is easily reached. Again, however, the long-term behaviour at low dose rates of these same fibers is uncertain.

5. TEST BEAM RESULTS

Measurements on candidate calorimeter sub-assemblies under the most realistic conditions possible are essential. Hertzog presented results of radiation damage tests on a small electromagnetic calorimeter. The calorimeter was exposed in steps to a total dose of 3 Megarad [at the electromagnetic shower peak]. Resolution and pulse height degraded on the day of exposure, but after four weeks it had completely recovered its initial resolution and half the initial pulse height.

This result is very encouraging, but such measurements could be made more relevant by increasing the test beam energy to 10^4 MeV from 10^2 MeV and, most importantly, extending the time of exposure to several months instead of only one day. It would be very useful to have measurements of realistic high-energy beam effects on different types of sub-assemblies, in order to 1) check how far the computed performance and measured performance are out of agreement, and 2) have a basis for quantative comparison of different design types.

6. TEST BEAMS

Such data will be slow in coming because of the lack of high energy test beams. We must make do therefore, with what is available. Majewski discusses methods of using electron beams to circumvent this problem and supplies a list of nearly a dozen facilities. Of those, however, only three are now, or will be, of >1 GeV energy, enough to realistically irradiate an assembled module. Most importantly, the availability of the beams for absolutely necessary long-term tests is not a given. High energy test beams remain a serious problem.

7.CONCLUSIONS

The Workshop brought into sharp focus the uncertainties and unresolved difficulties still faced by those who would construct a plastic-scintillator based calorimeter or tracker. There is still ambiguity about the role of the gas environment in annealing. An accurate model of long-term scintillator behaviour is an urgent necessity. Access to test beams needs to be ensured. Viable photodetectors matched to red emitting scintillator would add design flexibility.

But we have made great strides toward solving these problems. The Workshop brought a sense of optimism: if the question of long-term reliability can be satisfactorily resolved, then the present performance of the best scintilltors may suffice for the barrel region of the calorimeter.

LIST OF PARTICIPANTS

NAME	INSTITUTE
Jean Badier	Ecole Polytechnique
Maurizio Bertoldi	Florida State University
David Bintinger	SSC Laboratory
Zhao Chen	University of Florida
Roger Clough	Sandia National Laboratory
Martyn Corden	Florida State University
William Dunn	Quantum Research Services, Inc.
Jean Ernwein	CEN-Saclay
Tony Gabriel	Oak Ridge National Laboratory
Justin Gaynor	University of Florida
Nikos Giokaris	The Rockefeller University
Mark Goforth	Florida State University
Don Groom	Lawrence Berkeley Laboratory
Sharon Hagopian	Florida State University
Vasken Hagopian	Florida State University
Thomas Handler	University of Tennessee
David Hertzog	Univ. of Illinois at Urbana-Champaign
Charles Hurlbut	Bicron Corporation
Kurtis Johnson	Florida State University
Michael Kasha	Florida State University
Joel Kauffman	Philadelphia Coll. of Pharm. and Science
Joseph Lannutti	Florida State University
Stephen Linn	Florida State University
Robert Madden	Florida State University
Amelia Maio	LIP
Stan Majewski	CEBAF
Roger McNeil	Louisiana State University
Masa Mishina	Fermilab
Wayne Moser	Bicron Corporation
Adam Para	Fermilab
James Proudfoot	Argonne National Laboratory
Tohru Shimizu	Kuraray Corporation
James Thomaston	Florida State University
Horst Wahl	Florida State University
James Walker	University of Florida
Shield Wallace	Sandia National Laboratory
James White	Texas A & M
William Worstell	Boston University
Jin Xu	Florida State University
Kiyoshi Yasuoka	University of Tsukuba
Saul Youssef	Florida State University
Carl Zorn	CEBAF